



## Standard Test Methods for Determination of Fracture Toughness of Advanced Ceramics at Ambient Temperature<sup>1</sup>

This standard is issued under the fixed designation C 1421; the number immediately following the designation indicates the year of original adoption or, in the case of revision, the year of last revision. A number in parentheses indicates the year of last reapproval. A superscript epsilon ( $\epsilon$ ) indicates an editorial change since the last revision or reapproval.

### 1. Scope

1.1 These test methods cover the fracture toughness determination of  $K_{Ipb}$  (precracked beam test specimen),  $K_{Isc}$  (surface crack in flexure), and  $K_{Ivb}$  (chevron-notched beam test specimen) of advanced ceramics at ambient temperature. The fracture toughness values are determined using beam test specimens with a sharp crack. The crack is either a straight-through crack (pb), or a semi-elliptical surface crack (sc), or it is propagated in a chevron notch (vb).

NOTE 1—The terms bend(ing) and flexure are synonymous in these test methods.

1.2 These test methods determine fracture toughness values based on a force and crack length measurement (pb, sc), or a force measurement and an inferred crack length (vb). In general, the fracture toughness is determined from maximum force. Applied force and displacement or an alternative (for example, time) are recorded for the pb test specimen and vb test specimen.

1.3 These test methods are applicable to materials with either flat or with rising R-curves. The fracture toughness measured from stable crack extension may be different than that measured from unstable crack extension. This difference may be more pronounced for materials exhibiting a rising R-curve.

NOTE 2—One difference between the procedures in these test methods and test methods such as Test Method E 399, which measure fracture toughness,  $K_{Ic}$ , by one set of specific operational procedures, is that Test Method E 399 focuses on the start of crack extension from a fatigue precrack for metallic materials. In these test methods the test methods for advanced ceramics make use of either a sharp precrack formed via bridge flexure (pb) or via Knoop indent (sc) prior to the test, or a crack formed during the test (vb). Differences in test procedure and analysis may cause the values from each test method to be different. Therefore, fracture toughness values determined with these methods cannot be interchanged with  $K_{Ic}$  as defined in Test Method E 399 and may not be interchangeable with each other.

1.4 These test methods give fracture toughness values,  $K_{Ipb}$ ,

$K_{Isc}$ , and  $K_{Ivb}$ , for specific conditions of environment, test rate and temperature. The fracture toughness values,  $K_{Ipb}$ ,  $K_{Isc}$ , and  $K_{Ivb}$  for a material can be functions of environment, test rate and temperature.

1.5 These test methods are intended primarily for use with advanced ceramics which are macroscopically homogeneous. Certain whisker- or particle-reinforced ceramics may also meet the macroscopic behavior assumptions.

1.6 These test methods are divided into three major parts and related sub parts as shown below. The first major part is the main body and provides general information on the test methods described, the applicability to materials comparison and qualification, and requirements and recommendations for fracture toughness testing. The second major part is composed of annexes that provide procedures, test specimen design, precracking, testing, and data analysis for each method. Annex A1 describes suggested test fixtures, Annex A2 describes the pb method, Annex A3 describes the sc method, and Annex A4 describes the vb method. The third major part consists of three appendices detailing issues related to the fractography and precracking used for the sc method.

Main Body	Section
Scope	1
Referenced Documents	2
Terminology (including definitions, orientation and symbols)	3
Summary of Test Methods	4
Significance and Use	5
Interferences	6
Apparatus	7
Test Specimen Configurations, Dimensions and Preparations	8
General Procedures	9
Report (including reporting tables)	10
Precision and Bias	11
Annexes	
Test Fixture Geometries	A1
Special Requirements for Precracked Beam Method	A2
Special Requirements for Surface Crack in Flexure Method	A3
Special Requirements for Chevron Notch Flexure Method	A4
Appendices	
Precrack Characterization, Surface Crack in Flexure Method	X1
Complications in Interpreting Surface Crack in Flexure Precracks	X2
Alternative Precracking Procedure, Surface Crack in Flexure Method	X3

1.7 Values expressed in these test methods are in accordance with the International System of Units (SI) and Practice E 380.

1.8 *This standard does not purport to address all of the safety concerns, if any, associated with its use. It is the*

<sup>1</sup> This test method is under the jurisdiction of ASTM Committee C28 on Advanced Ceramics and is the direct responsibility of Subcommittee C28.01 on Properties and Performance.

Current edition approved Oct. 10, 2001. Published January 2002. Originally published as C 1421 - 99. Last previous edition C 1421 - 01a.

responsibility of the user of this standard to establish appropriate safety and health practices and determine the applicability of regulatory limitations prior to use.

## 2. Referenced Documents

### 2.1 ASTM Standards:

- C 1161 Test Method for Flexural Strength of Advanced Ceramics at Ambient Temperature<sup>2</sup>
- C 1322 Practice for Fractography and Characterization of Fracture Origins in Advanced Ceramics<sup>2</sup>
- E 4 Practices for Force Verification of Testing Machines<sup>3</sup>
- E 112 Test Methods for Determining Average Grain Size<sup>3</sup>
- E 177 Practice for Use of the Terms Precision and Bias in ASTM Test Methods<sup>4</sup>
- E 337 Test Method for Measuring Humidity with a Psychrometer (the Measurement of Wet- and Dry-Bulb Temperatures)<sup>5</sup>
- E 399 Test Method for Plane-Strain Fracture Toughness of Metallic Materials<sup>3</sup>
- E 691 Practice for Conducting an Interlaboratory Study to Determine the Precision of a Test Method<sup>4</sup>
- E 740 Practice for Fracture Testing with Surface-Crack Tension Specimens<sup>3</sup>
- E 1823 Terminology Relating to Fracture Testing<sup>3</sup>
- IEEE/ASTM SI 10 Standard for Use of the International System of Units (SI) (The Modern Metric System)<sup>6</sup>
- 2.2 Reference Material:
- NIST SRM 2100 Fracture Toughness of Ceramics<sup>7</sup>

## 3. Terminology

### 3.1 Definitions:

3.1.1 The terms described in Terminology E 1823 are applicable to these test methods. Appropriate sources for each definition are provided after each definition in parentheses.

3.1.2 *crack extension resistance*,  $K_R[FL^{-3/2}]$ ,  $G_R[FL^{-1}]$ , or  $J_R[FL^{-1}]$ ,—a measure of the resistance of a material to crack extension expressed in terms of the stress-intensity factor,  $K$ , strain energy release rate,  $G$ , or values of  $J$  derived using the J-integral concept. **(E 1823)**

3.1.3 *fracture toughness*—a generic term for measures of resistance of extension of a crack. **(E 399, E 1823)**

3.1.4 *R-curve*—a plot of crack-extension resistance as a function of stable crack extension.

3.1.5 *slow crack growth (SCG)*—sub critical crack growth (extension) which may result from, but is not restricted to, such mechanisms as environmentally-assisted stress corrosion or diffusive crack growth.

3.1.6 *stress-intensity factor*,  $K [FL^{-3/2}]$ —the magnitude of the ideal-crack-tip stress field (stress field singularity) for a particular mode in a homogeneous, linear-elastic body. **(E 1823)**

### 3.2 Definitions of Terms Specific to This Standard:

3.2.1 *back-face strain*—the strain as measured with a strain gage mounted longitudinally on the compressive surface of the test specimen, opposite the crack or notch mouth (often this is the top surface of the test specimen as tested)

3.2.2 *crack depth*,  $a [L]$ —in surface-cracked test specimens, the normal distance from the cracked beam surface to the point of maximum penetration of crack front in the material.

3.2.3 *crack orientation*—a description of the plane and direction of a fracture in relation to a characteristic direction of the product. This identification is designated by a letter or letters indicating the plane and direction of crack extension. The letter or letters represent the direction normal to the crack plane and the direction of crack propagation.

3.2.3.1 *Discussion*—The characteristic direction may be associated with the product geometry or with the microstructural texture of the product.

3.2.3.2 *Discussion*—The fracture toughness of a material may depend on the orientation and direction of the crack in relation to the material anisotropy, if such exists. Anisotropy may depend on the principal pressing directions, if any, applied during green body forming (for example, uniaxial or isopressing, extrusion, pressure casting) or sintering (for example, uniaxial hot-pressing, hot isostatic pressing). Thermal gradients during firing can also lead to microstructural anisotropy.

3.2.3.3 *Discussion*—The crack plane is defined by letter(s) representing the direction normal to the crack plane as shown in Fig. 1, Fig. 2, and Fig. 3. The direction of crack extension is defined also by the letter(s) representing the direction parallel to the characteristic direction (axis) of the product as illustrated in Fig. 1b, Fig. 2b and Fig. 3b.

HP = hot-pressing direction (See Fig. 1)

EX = extrusion direction (See Fig. 2)

AXL = axial, or longitudinal axis (if HP or EX are not applicable)

R = radial direction (See Fig. 1, Fig. 2 and Fig. 3)

C = circumferential direction (See Fig. 1, Fig. 2 and Fig. 3)

R/C = mixed radial and circumferential directions (See Fig. 3b)

3.2.3.4 *Discussion*—For a rectangular product, R and C may be replaced by rectilinear axes x and y, corresponding to two sides of the plate.

3.2.3.5 *Discussion*—Depending on how test specimens are sliced out of a ceramic product, the crack plane may be circumferential, radial, or a mixture of both as shown in Fig. 3.

3.2.3.6 Identification of the plane and direction of crack extension is recommended. The plane and direction of crack extension are denoted by a hyphenated code with the first letter(s) representing the direction normal to the crack plane, and the second letter(s) designating the expected direction of crack extension. See Fig. 1, Fig. 2 and Fig. 3.

3.2.3.7 *Discussion*—In many ceramics, specification of the crack plane is sufficient.

3.2.3.8 Isopressed products, amorphous ceramics, glasses and glass ceramics are often isotropic, and crack plane orientation has little effect on fracture toughness. Nevertheless, the designation of crack plane relative to product geometry is recommended. For example, if the product is isopressed (either cold or hot) denote the crack plane and direction relative to the axial direction of the product. Use the same designation

<sup>2</sup> Annual Book of ASTM Standards, Vol 15.01.

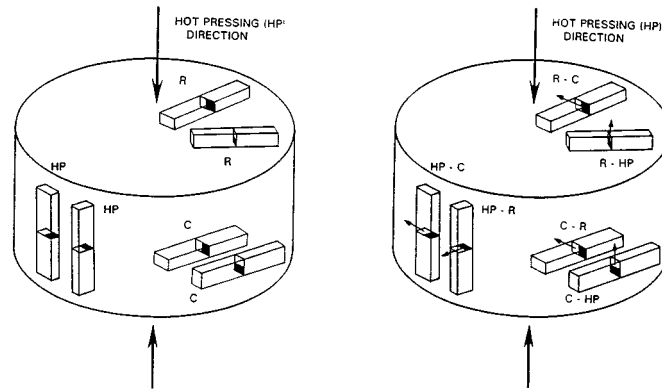
<sup>3</sup> Annual Book of ASTM Standards, Vol 03.01.

<sup>4</sup> Annual Book of ASTM Standards, Vol 14.02.

<sup>5</sup> Annual Book of ASTM Standards, Vol 07.01, 11.03, and 15.09.

<sup>6</sup> Annual Book of ASTM Standards, Vol 14.04.

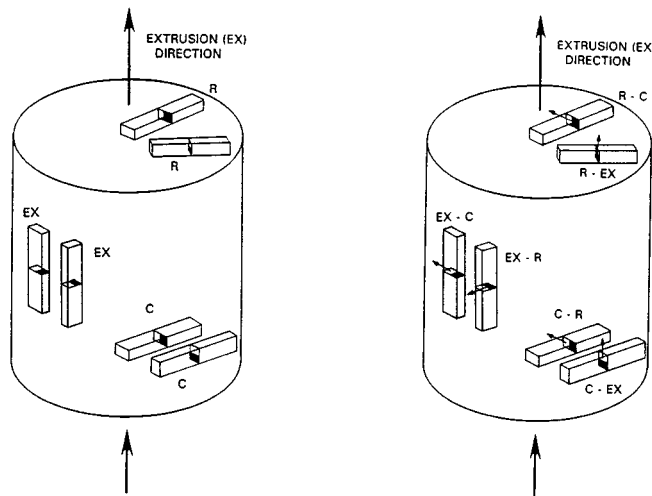
<sup>7</sup> Available from National Institute of Standards and Technology, Gaithersburg, MD 20899.



a) Crack plane designated, only b) Crack plane and direction of crack extension designated

NOTE 1—Precracked beam test specimens are shown as examples. The small arrows denote the direction of crack growth.

**FIG. 1 Crack Plane Orientation Code for Hot-Pressed Products**



a) Crack plane designated, only b) Crack plane and direction of crack extension designated

NOTE 1—Precracked beam test specimens are shown as examples. The small arrows denote the direction of crack growth.

**FIG. 2 Crack Plane Orientation Code for Extruded Products**

scheme as shown in Figs. 1 and 2, but with the letters “AXL” to denote the axial axis of the product.

3.2.3.9 If there is no primary product direction, reference axes may be arbitrarily assigned but must be clearly identified.

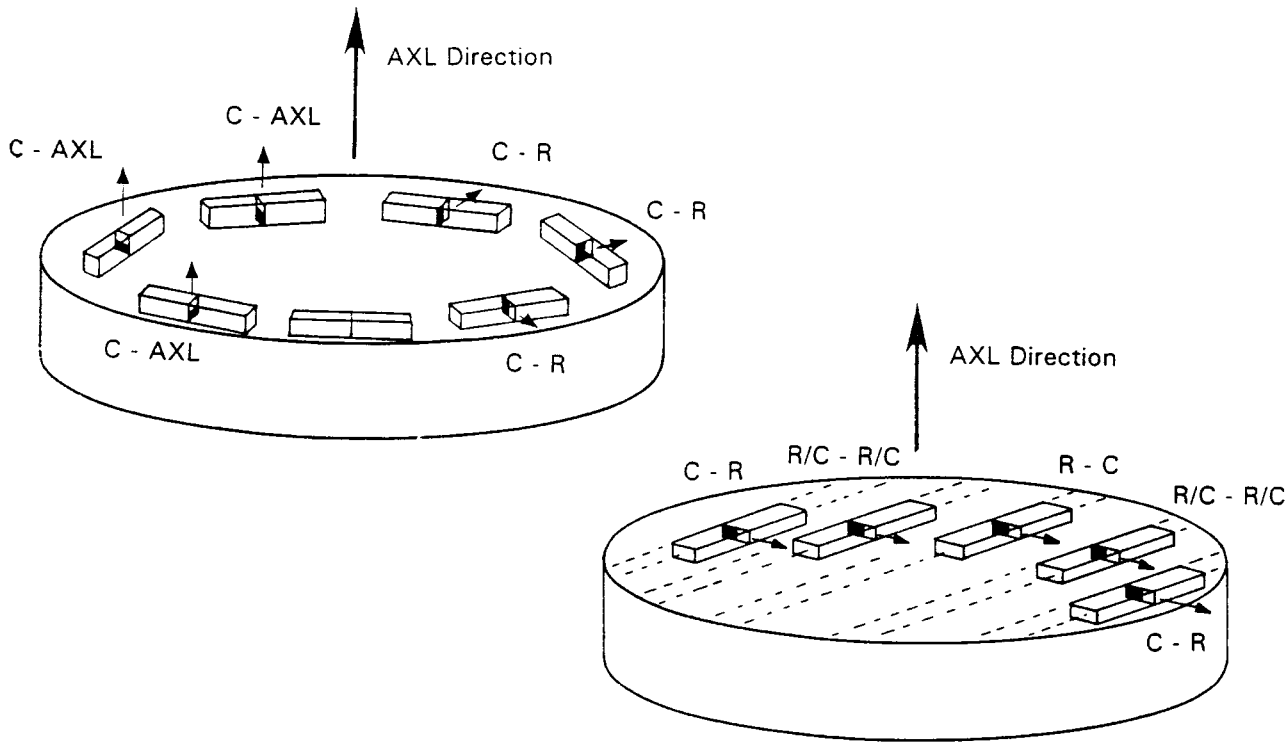
3.2.4 *critical crack size*  $[L]$ —in these test methods, the crack size at which maximum force and catastrophic fracture occur in the precracked beam (see Fig. 4) and the surface crack in flexure (see Fig. 5) configurations. In the chevron-notched test specimen (see Fig. 6) this is the crack size at which the stress intensity factor coefficient,  $Y^*$ , is at a minimum or equivalently, the crack size at which the maximum force would occur in a linear elastic, flat R-curve material.

3.2.5 *four-point - 1/4 point flexure*—flexure configuration where a beam test specimen is symmetrically loaded at two

locations that are situated one quarter of the overall span, away from the outer two support bearings (see Fig. A1.1) (C 1161)

3.2.6 *fracture toughness*  $K_{Ipb}[FL^{-3/2}]$ —the measured stress intensity factor corresponding to the extension resistance of a straight-through crack formed via bridge flexure of a sawn notch or Vickers or Knoop indentation(s). The measurement is performed according to the operational procedure herein and satisfies all the validity requirements. (See Annex A2).

3.2.7 *fracture toughness*  $K_{Isc}$  or  $K_{Isc}^*[FL^{-3/2}]$ —the measured ( $K_{Isc}$ ) or apparent ( $K_{Isc}^*$ ) stress intensity factor corresponding to the extension resistance of a semi-elliptical crack formed via Knoop indentation, for which the residual stress field due to indentation has been removed. The measurement is performed according to the operational procedure herein and



- a) Specimens cut circumferentially  
All crack planes are "C," but  
direction of crack extension  
is either radial, "R" or axial, "AXL"
- b) Specimens prepared from parallel slices.  
Crack planes and direction of crack extension  
are "R" or "C" or mixed depending on the  
location

NOTE 1—The R/C mix shown in b) is a consequence of the parallel slicing of the test specimens from the product.

NOTE 2—Precracked beam test specimens are shown as examples. The small arrows denote the direction of crack growth.

FIG. 3 Code for Crack Plane and Direction of Crack Extension in Test Specimens with Axial Primary Product Direction

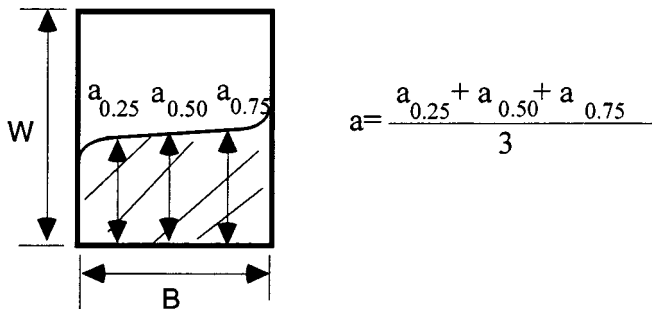


FIG. 4 Cross Section of a pb Test Specimen Showing the Precrack Configuration ( $a_{0.25}$ ,  $a_{0.50}$ ,  $a_{0.75}$  are the Points for Crack Length Measurements)

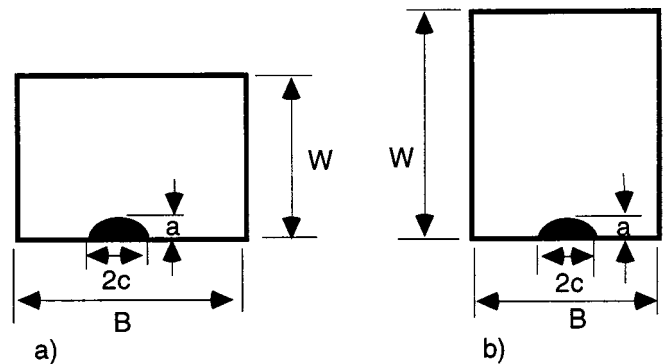


FIG. 5 a and b Cross Section of sc Test Specimens Showing the Precrack Configurations for Two Orientations

satisfies all the validity requirements. (See Annex A3).

3.2.8 *fracture toughness*  $K_{Ivb}[FL^{-3/2}]$ —the measured stress intensity factor corresponding to the extension resistance of a stably-extending crack in a chevron-notched test specimen. The measurement is performed according to the operational procedure herein and satisfies all the validity requirements. (See Annex A4).

3.2.9 *minimum stress-intensity factor coefficient*,  $Y^*_{min}$ —the minimum value of  $Y^*$  determined from  $Y^*$  as a function of dimensionless crack length,  $\alpha = a/W$ .

3.2.10 *pop-in*—in these test methods, the sudden formation or extension of a crack without catastrophic fracture of the test specimen, apparent from a force drop in the applied force-displacement curve. Pop-in may be accompanied by an audible sound or other acoustic energy emission.

3.2.11 *precrack*—a crack that is intentionally introduced into the test specimen prior to testing the test specimen to fracture.

3.2.12 *small crack*—a crack is defined as being small when all physical dimensions (in particular, with length and depth of

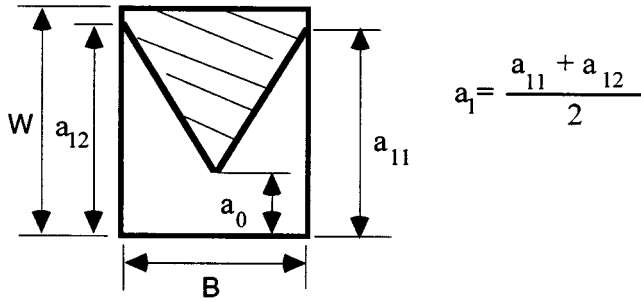


FIG. 6 Cross Section of a vb Test Specimen Showing the Notch Configuration

a surface crack) are small in comparison to a relevant microstructural scale, continuum mechanics scale, or physical size scale. The specific physical dimensions that define “small” vary with the particular material, geometric configuration, and loadings of interest. (E 1823)

3.2.13 *stable crack extension*—controllable, time-independent, noncritical crack propagation.

3.2.13.1 *Discussion*—The mode of crack extension (stable or unstable) depends on the compliance of the test specimen and test fixture; the test specimen and crack geometries; R-curve behavior of the material; and susceptibility of the material to slow crack growth.

3.2.14 *three-point flexure*—flexure configuration where a beam test specimen is loaded at a location midway between two support bearings (see Fig. A1.2) (C 1161)

3.2.15 *unstable crack extension*—uncontrollable, time-independent, critical crack propagation.

### 3.3 Symbols:

3.3.1  $a$ —as used in these test methods, crack depth, crack length, crack size.

3.3.2  $a_o$ —as used in these test methods, chevron tip dimension, vb method, Fig. 6 and Fig. A4.1.

3.3.3  $a_1$ —as used in these test methods, chevron dimension, vb method, Fig. 6, ( $a_1 = (a_{11} + a_{12})/2$ ).

3.3.4  $a_{11}$ —as used in these test methods, chevron dimension, vb method, Fig. 6 and Fig. A4.1.

3.3.5  $a_{12}$ —as used in these test methods, chevron dimension, vb method, Fig. 6 and Fig. A4.1.

3.3.6  $a_{0.25}$ —as used in these test methods, crack length measured at 0.25B, pb method, Fig. 4.

3.3.7  $a_{0.50}$ —as used in these test methods, crack length measured at 0.5B, pb method, Fig. 4.

3.3.8  $a_{0.75}$ —as used in these test methods, crack length measured at 0.75B, pb method, Fig. 4.

3.3.9  $a/W$ —normalized crack size.

3.3.10  $B$ —as used in these test methods, the side to side dimension of the test specimen perpendicular to the crack length (depth) as shown in Fig. 4, Fig. 5, and Fig. 6.

3.3.11  $c$ —as used in these test methods, crack half width, sc method, see Fig. 5 and Fig. A3.2.

3.3.12  $d$ —as used in these test methods, length of long diagonal for a Knoop indent, length of a diagonal for a Vickers indent, sc method.

3.3.13  $E$ —elastic modulus.

3.3.14  $f(a/W)$ —function of the ratio  $a/W$ , pb method, four-point flexure, Eq A2.6.

3.3.15  $F$ —indent force, sc method.

3.3.16  $g(a/W)$ —function of the ratio  $a/W$ , pb method, three-point flexure, Eq A2.2 and Eq A2.4.

3.3.17  $h$ —as used in this standard, depth of Knoop or Vickers indent, sc method, Eq A3.1.

3.3.18  $H_1(a/c, a/W)$ —a polynomial in the stress intensity factor coefficient, for the precrack periphery where it intersects the test specimen surface, sc method, Eq A3.7.

3.3.19  $H_2(a/c, a/W)$ —a polynomial in the stress intensity factor coefficient, for the deepest part of a surface crack, sc method, see Eq A3.5.

3.3.20  $K_I$ —stress intensity factor, Mode I.

3.3.21  $K_{Ipb}$ —fracture toughness, pb method, Eq A2.1 and Eq A2.3.

3.3.22  $K_{Isc}$ —fracture toughness, sc method, Eq A3.9.

3.3.23  $K_{Ivb}$ —fracture toughness, vb method, Eq A4.1.

3.3.24  $L$ —test specimen length, Figs. A2.1 and A3.1.

3.3.25  $L1, L2$ —precracking fixture dimensions, pb method, Fig. A2.2.

3.3.26  $M(a/c, a/W)$ —a polynomial in the stress intensity factor coefficient, sc method, see Eq A3.4.

3.3.27  $P$ —force.

3.3.28  $P_{max}$ —force maximum.

3.3.29  $Q(a/c)$ —a polynomial function of the surface crack ellipticity, sc method, Eq A3.3.

3.3.30  $S(a/c, a/W)$ —factor in the stress intensity factor coefficient, sc method, Eq A3.8.

3.3.31  $S_o$ —outer span, three- or four-point test fixture. Figs. A1.1 and A1.2.

3.3.32  $S_i$ —inner span, four-point test fixture, Fig. A1.1.

3.3.33  $t$ —notch thickness, pb and vb method.

3.3.34  $W$ —the top to bottom dimension of the test specimen parallel to the crack length (depth) as shown in Fig. 4, Fig. 5, and Fig. 6.

3.3.35  $Y$ —stress intensity factor coefficient.

3.3.36  $Y^*$ —stress intensity factor coefficient for vb method.

3.3.37  $Y_{max}$ —maximum stress intensity factor coefficient occurring around the periphery of an assumed semi-elliptical precrack, sc method

3.3.38  $Y_{min}^*$ —minimum stress intensity factor coefficient, vb method, Eq A4.2-A4.5

3.3.39  $Y_d$ —stress intensity factor coefficient at the deepest part of a surface crack, sc method, Eq A3.2

3.3.40  $Y_s$ —stress intensity factor coefficient at the intersection of the surface crack with the test specimen surface, sc method, Eq A3.6

## 4. Summary of Test Methods

4.1 These methods involve application of force to a beam test specimen in three- or four-point flexure. The test specimen either contains a sharp crack initially or develops one during loading. The equations for calculating the fracture toughness have been established on the basis of elastic stress analyses of the test specimen configurations described for each test method.

4.2 *Precracked Beam Method*—A straight-through precrack is created in a beam test specimen via the bridge-flexure technique. In this technique the precrack is extended from median cracks associated with one or more Vickers indents or



a shallow sawed notch. The fracture force of the precracked test specimen as a function of displacement or alternative (for example, time, back-face strain, or actuator displacement) in three- or four-point flexure is recorded for analysis. The fracture toughness,  $K_{Ipb}$ , is calculated from the fracture force, the test specimen size and the measured precrack size. Background information concerning the basis for development of this test method may be found in Refs. (1)<sup>8</sup> and (2).

**4.3 Surface Crack in Flexure Method**—A beam test specimen is indented with a Knoop indenter and polished (or hand ground), while maintaining surface parallelism, until the indent and associated residual stress field are removed. The fracture force of the test specimen is determined in four-point flexure and the fracture toughness,  $K_{Isc}$ , is calculated from the fracture force, the test specimen size, and the measured precrack size. Background information concerning the basis for development of this test method may be found in Refs. (3) and (4).

**4.4 Chevron-Notched Beam Method**—A chevron-notched beam is loaded in either three- or four-point flexure. Applied force versus displacement or an alternative (for example, time, back-face strain, or actuator displacement) is recorded in order to detect unstable fracture, since the test is invalid for unstable conditions. The fracture toughness,  $K_{Ivb}$ , is calculated from the maximum force applied to the test specimen after extension of the crack in a stable manner. Background information concerning the basis for the development of this test method may be found in Refs. (5) and (6).

**NOTE 3**—The fracture toughness of many ceramics varies as a function of the crack extension occurring up to the relevant maximum force. The actual crack extension to achieve the minimum stress intensity factor coefficient ( $Y^*_{min}$ ) of the chevron notch configurations described in this method is 0.68 to 0.93 mm. This is likely to result in a fracture toughness value in the upper region of the R-curve.

## 5. Significance and Use

**5.1** These test methods may be used for material development, material comparison, quality assessment, and characterization.

**5.2** The pb and the vb fracture toughness values provide information on the fracture resistance of advanced ceramics containing large sharp cracks, while the sc fracture toughness value provides this information for small cracks comparable in size to natural fracture sources.

**NOTE 4**—Cracks of different sizes may be used for the sc method. If the fracture toughness values vary as a function of the surface crack size it can be expected that  $K_{Isc}$  will differ from  $K_{Ipb}$  and  $K_{Ivb}$ .

## 6. Interferences

**6.1 R-curve**—The microstructural features of advanced ceramics can cause rising R-curve behavior. For such materials the three test methods are expected to result in different fracture toughness values. These differences are due to the amount of crack extension prior to the relevant maximum test force,  $P_{max}$ , (see 9.8), or they are due to the details of the precracking methods. For materials tested to date the fracture

toughness values generally increase in the following order:  $K_{Isc}$ ,  $K_{Ipb}$ ,  $K_{Ivb}$  (7). However, there is insufficient experience to extend this statement to all materials. In the analysis of the vb method it is assumed that the material has a flat (no) R-curve. If significant R-curve behavior is suspected, then the sc method should be used for estimates of small-crack fracture toughness, whereas the vb test may be used for estimates of longer-crack fracture toughness. The pb fracture toughness may reflect either short- or long-crack length fracture toughness depending on the precracking conditions. For materials with a flat (no) R-curve the values of  $K_{Ipb}$ ,  $K_{Isc}$ , and  $K_{Ivb}$  are expected to be similar.

**6.2 Time-Dependent Phenomenon and Environmental Effects**—The values of  $K_{Ipb}$ ,  $K_{Isc}$ ,  $K_{Ivb}$ , for any material can be functions of test rate because of the effects of temperature or environment. Static forces applied for long durations can cause crack extension at  $K_I$  values less than those measured in these methods. The rate of, and level at which, such crack extension occurs can be changed by the presence of an aggressive environment, which is material specific. This time-dependent phenomenon is known as slow crack growth (SCG) in the ceramics community. SCG can be meaningful even for the relatively short times involved during testing and can lead to measured fracture toughness values less than the inherent resistance in the absence of environmental effects. This effect may be significant even at ambient conditions and can often be minimized or emphasized by selecting a fast or slow test rate, respectively, or by changing the environment. The recommended testing rates specified are an attempt to limit environmental effects.

**6.3 Stability**—The stiffness of the test set-up can affect the fracture toughness value. This standard permits measurements of fracture toughness under either unstable (sc, pb) or stable (sc, pb, vb) conditions. Stiff testing systems will promote stable crack extension. A stably-extending crack may give somewhat lower fracture toughness values (8,9).

**6.4** Processing details, service history, and environment may alter the fracture toughness of the material.

## 7. Apparatus

**7.1 Testing**—Test the test specimens in a testing machine that has provisions for autographic recording of force applied to the test specimen versus either test specimen load or centerline deflection or time. The accuracy of the testing machine shall be in accordance with Practice E 4.

**7.2 Deflection Measurement**—When determined, measure test specimen deflection for the pb and vb close to the crack. The deflection gauge should be capable of resolving  $1 \times 10^{-3}$  mm (1  $\mu$ m) while exerting a contacting force of less than 1 % of the maximum test force,  $P_{max}$ .

**NOTE 5**—If actuator displacement (stroke) is used to infer deflection of the test specimen for the purposes of assessing stability, caution is advised. Actuator displacement (stroke), although sometimes successfully used for this purpose (9), may not be as sensitive to changes of fracture behavior in the test specimen as measurements taken on the test specimen itself, such as back-face strain, load-point displacement, or displacement at the crack plane (10).

**7.3 Recording Equipment**—Provide a means for automatically recording the applied force-displacement or load-time test

<sup>8</sup> The boldface numbers given in parentheses refer to a list of references at the end of the text.

record, (such as a X-Y recorder). For digital data acquisition sampling rates of 500 Hz or greater are recommended.

**7.4 Fixtures**—Use four-point or three-point test fixtures to force the pb and vb test specimens. Use four-point test fixtures only to force the sc test specimens. In addition, use a precracking fixture for the pb method.

**NOTE 6**—Hereafter in this document the term four-point flexure will refer to the specific case of  $\frac{1}{4}$ -(that is, quarter) point flexure.

**7.4.1** The schematic of a four-point test fixture is shown in Fig. A1.1, as specified in Test Method C 1161 where the recommended outer and inner spans are  $S_o = 40$  mm and  $S_i = 20$  mm, respectively. The minimum outer and inner spans shall be  $S_o = 20$  mm and  $S_i = 10$  mm, respectively. The outer rollers shall be free to roll outwards and the inner rollers shall be free to roll inwards. The rolling movement minimizes frictional restraint effects which can cause flexure errors of 3 to 20 %. Place the rollers initially against their stops and hold them in position by low-tension springs (such as rubber bands). Roller pins shall have a hardness of 40 Rockwell C or greater. Other fixtures are acceptable, however, roller pins shall be free to roll and meet the criteria specified in 7.4.2.

**7.4.2** The length of each roller shall be at least three times the test specimen dimension, B. The roller diameter shall be  $4.5 \pm 0.5$  mm. The rollers shall be parallel to each other within 0.015 mm over either the length of the roller or a length of 3B or greater.

**7.4.3** If the test specimen parallelism requirements set forth in Fig. A2.1 and Fig. A3.1 are not met, use an alternate fully-articulating fixture.

**7.4.4** The fixture shall be capable of maintaining the test specimen alignment to the tolerances specified in 9.6.

**7.4.5** A suggested three-point test fixture design is shown in Fig. A1.2. Choose the outer support span,  $S_o$ , such that  $4 \leq \frac{S_o}{W} \leq 10$ , although  $S_o$  should not be less than 16 mm. For limits of validity of  $S_o$ , refer to the appropriate appendix. The outer two rollers shall be free to roll outwards to minimize friction effects. The middle flexure roller shall be fixed. Alternatively, a rounded knife edge with diameter in accordance with 7.4.2 may be used in place of the middle roller.

**NOTE 7**—If stable crack extension is desired in the pb test, then displacement control mode and a stiff test system and load train may be required. The specific stiffness requirements are dependent on the test specimen dimensions, elastic modulus (E) and the precrack length (see A2.1.1.2 and Refs. (8) and (9).) A test system compliance of less than or equal to  $3.3 \times 10^{-8}$  m/N (including load cell and fixtures) may be required for a typical stable pb test. (See Refs. (8) and (9).)

**NOTE 8**—A stiff test system with displacement control and a stiff load train may be required to obtain stable crack extension for the vb test (Fig. A4.3b or Fig. A4.3c). Without such stable crack extension the test is invalid (Fig. A4.3a). See also A4.3.6. A test system compliance of less than or equal to  $4.43 \times 10^{-5}$  m/N (including load cell and fixtures) is adequate for most vb tests.

**7.5 Dimension-Measuring Devices**—Micrometers and other devices used for measuring test specimen dimensions shall be accurate and precise to 0.0025 mm or better. Flat, anvil-type micrometers with resolutions of 0.0025 or less shall be used for test specimen dimensions. Ball-tipped or sharp-anvil micrometers are not recommended as they may damage the test

specimen surface by inducing localized cracking. Non-contacting (for example, optical comparator, light microscopy, etc.) measurements are recommended for crack, pre-crack or notch measurements, or all of these.

## 8. Test Specimen Configurations, Dimensions and Preparation

**8.1 Test Specimen Configuration**—Three precrack configurations are equally acceptable: a straight-through pb-crack, a semi-elliptical sc-crack, or a vb-chevron notch. These configurations are shown in Fig. 4, Fig. 5, and Fig. 6. Details of the crack geometry are given in the Annexes (Annex A2 for the pb, Annex A3 for the sc, and Annex A4 for the vb)

**8.2 Test Specimen Dimensions**—Specific dimensions, tolerances and finishes along with additional test specimen geometries for each method are detailed in the appropriate annex.

**NOTE 9**—A typical “plastic” (or deformation) zone, if such exists, is no greater than a fraction of a micrometre in most ceramics, thus the specified sizes are large enough to meet generally-accepted plane strain requirements at the crack tip (see Test Method E 399).

**8.3 Test Specimen Preparation**—Machining aspects unique to each test method are contained in the appropriate annex.

## 9. General Procedures

**9.1 Number of Tests**—Complete a minimum of four valid tests for each material and testing condition.

**9.2 Valid Tests**—A valid individual test is one which meets all the following requirements: all the general testing requirements of this standard as listed in 9.2.1, and all the specific testing requirements for a valid test of the particular test method as specified in the appropriate annex.

**9.2.1** A valid test shall meet the following general requirements in addition to the specific requirements of the particular test (A2.6, A3.6 or A4.6):

**9.2.1.1** Test machine shall have provisions for autographic recording of force versus deflection or time, and the test machine shall have an accuracy in accordance with Practice E 4 (7.1).

**9.2.1.2** Test fixtures shall comply with specifications of 7.4.

**9.2.1.3** Dimension-measuring devices shall comply with specifications of 7.5.

**9.2.1.4** Test specimens shall be aligned to comply with 9.6.

**9.2.1.5** Test rate shall be in conformance with 9.7.

**9.3 Environmental Effects**—If susceptibility to environmental degradation, such as slow crack growth, is a concern, tests should be performed and reported at two different test rates, or in appropriately different environments

**NOTE 10**—If used, the two test rates should differ by two to three orders of magnitude (or greater). Alternatively, choose different environments such that the expected effect is small in one case (for example, inert dry nitrogen) and large in the other case (that is, water vapor). If an effect of the environment is detected, select the fracture toughness values measured at the greater test rates or in the inert environment.

**9.4 R-curve**—When rising R-curve behavior is to be documented, two different test methods with different amounts of stable crack extension should be used.

**NOTE 11**—The pb and sc tests typically have less stable crack extension than the vb test.

**9.5 Test Specimen Measurements**—Measure and report all applicable test specimen dimensions to 0.002 mm. For a valid test the dimensions shall conform to the tolerances shown in the applicable figures and to the requirements in the specific annexes.

**9.6 Test Specimen Alignment**—Place the test specimen in the three- or four-point flexure fixture. Align the test specimen so that it is centered directly below the axis of the force application.

**9.6.1 Three-point Flexure**—pb and vb methods: The plane of the crack shall be centered under the middle roller within 0.5 mm. Measure the span within 0.5 % of  $S_0$ . Align the center of the middle roller so that its line of action shall pass midway between the two outer rollers within 0.1 mm. Seat the displacement indicator close to the crack plane. Alternatively, use actuator (or crosshead) displacement, back-face strain, or a time sweep.

**NOTE 12**—For short spans (for example,  $S_0=16$  mm) and  $S_0/W=4.0$  in three-point flexure using the pb method, errors of up to 3 % in determining the critical mode I stress intensity factor may occur because of misalignment of the middle roller, misalignment of the support span or angularity of the precrack at the extremes of the tolerances allowed in 9.6.1 (11, 12).

**9.6.2 Four-Point Flexure - pb, sc, and vb Methods**—The plane of the crack shall be located within 1.0 mm of the midpoint between the two inner rollers,  $S_i$ . Measure the inner and outer spans to within 0.1 mm. Align the midpoint of the two inner rollers relative to the midpoint of the two outer rollers to within 0.1 mm. For the pb and vb methods, seat the displacement indicator close to the crack plane. Alternatively, use actuator (or crosshead) displacement (stroke), back-face strain or a time sweep.

**9.7 Test Rate**—Test the test specimen so that one of the test rates determined in 9.3 will result in a rate of increase in stress intensity factor between 0.1 and 2.75 MPa  $\sqrt{m/s}$ . Applied force, or displacement (actuator or stroke) rates, or both, corresponding to these stress intensity factor rates are discussed in the appropriate annex. Other test rates are permitted if environmental effects are suspected in accordance with 9.3.

**9.8 Force Measurement**—Measure the relevant maximum test force,  $P_{max}$ .

**9.8.1** For the pb and sc test methods, the relevant maximum force is the greatest force occurring during the test.

**9.8.2** For the vb test method, the relevant maximum force is measured as the maximum force occurring during the stable crack extension (See Fig. A4.3b and c). Ignore the maximum force due to a pop-in or crack jump. (See Fig. A4.3b). In some cases the relevant maximum force may not be the greatest force occurring during the test.

**9.9 Humidity**—Measure the temperature and humidity according to Test Method E 337.

**9.10 Test Specimen Examination**—On completion of the test, separate the test specimen halves and inspect the fracture surfaces for out-of-plane fracture, crack shape irregularities or any other imperfection that may have influenced the test result.

**9.11 Dimension Measurement**—Measure the crack or precrack dimensions of the pb or sc test specimen after fracture as specified in the appropriate annex.

## 10. Report

**10.1** For each test specimen report the following information:

**10.1.1** Test specimen identification,

**10.1.2** Form of product tested, and materials processing information, if available,

**10.1.3** Mean grain size, if available, by Test Method E 112 or other appropriate method,

**10.1.4** Environment of test, relative humidity, temperature, and crack plane orientation,

**10.1.5** Test specimen dimensions:  $B$  and  $W$ ,

**10.1.5.1** For the pb test specimen crack length,  $a$ , and notch thickness,  $t$ , if applicable,

**10.1.5.2** For the sc test specimen the crack dimensions  $a$  and  $2c$ ,

**10.1.5.3** For the vb test specimen the notch parameters,  $a_0$  and  $a_{11}$  and  $a_{12}$  and the notch thickness,  $t$ ,

**10.1.6** Test fixture specifics,

**10.1.6.1** Whether the test was in three- or four-point flexure,

**10.1.6.2** Outer span,  $S_0$ , and inner span (if applicable),  $S_i$ ,

**10.1.7** Applied force or displacement rate,

**10.1.8** Measured inclination of the crack plane as specified in the appropriate annex,

**10.1.9** Relevant maximum test force,  $P_{max}$ , as specified in the appropriate annex,

**10.1.10** Testing diagrams (for example, applied force vs. displacement) as required,

**10.1.11** Number of test specimens tested and the number of valid tests,

**10.1.12** Fracture toughness value with statement of validity,

**10.1.13** Additional information as required in the appropriate annex, and

**10.2** Mean and standard deviation of the fracture toughness for each test method used.

**10.3 Reporting Templates**—Suggested reporting templates for conveniently listing pertinent data and results for the three different test methods are shown in Fig. 7, Fig. 8, and Fig. 9.

## 11. Precision and Bias

**11.1 Precision**—The precision of a fracture toughness measurement is a function of the precision of the various measurements of linear dimensions of the test specimen and test fixtures, and the precision of the force measurement. The within-laboratory (repeatability) and between-laboratory (reproducibility) precisions of some of the fracture toughness procedures in this test method have been determined from inter-laboratory test programs (13, 14). For specific dependencies of each test method, refer to the appropriate annex.

**11.2 Bias**—Standard Reference Material (SRM) 2100 from the National Institute of Standards and Technology may be used to check for laboratory test result bias. The laboratory average value may be compared to the certified reference value of fracture toughness. SRM 2100 is a set of silicon nitride beam test specimens for which the mean fracture toughness is 4.57 MPa $\sqrt{m}$  and is certified to within 2.3 % at a 95 % confidence level. The last line of Table 2 in this standard includes some results obtained on SRM 2100 test specimens. Additional data (not shown) confirms that virtually identical



**TABLE 1 Fracture Toughness Values of Sintered Silicon Carbide (Hexoloy SA) in MPa  $\sqrt{m}$** 

(n) = Number of test specimens tested  
 $\pm$  = 1 Standard Deviation  
 ? = quantity unknown

Precracked Beam (pb)	Surface Crack in Flexure (sc)	Chevron-Notch (vb)	Ref
2.54 $\pm$ 0.20 (3)	2.69 $\pm$ 0.08 (6) <sup>A</sup>	2.62 $\pm$ 0.06 (6) (A config.) 2.68 $\pm$ 0.03 (a) (B config.)	<sup>A,B</sup> using II-UW material, vintage 1985
2.58 $\pm$ 0.08 (4)	2.76 $\pm$ 0.08 (4) <sup>A</sup>	2.61 $\pm$ 0.05 (6) (A config.) 2.46 $\pm$ 0.03 (5) (C config.)	<sup>A,B</sup> using JAS material, vintage 1980
...	3.01 $\pm$ 0.35 (3) <sup>C</sup>	2.91 $\pm$ 0.31 (3) (B config.)	<sup>D</sup>

<sup>A</sup>G.D. Quinn and J.A. Salem, "Effect of Lateral Cracks Upon Fracture Toughness Determined by the Surface crack in Flexure Method," *J. Am. Ceram. Soc.*, in press, July 2001

<sup>B</sup>J.A. Salem, L.J. Ghosn, M.G. Jenkins, and G. D. Quinn, "Stress Intensity Factor Coefficients for Chevron-Notched Flexure Specimens," *Ceramic Engineering and Science Proceedings*, 20 [3] 1999, pp. 503–512.

<sup>C</sup>This data set may have been susceptible to overestimation of the sc fracture toughness due to the interference of vestigial lateral cracks.

<sup>D</sup>A. Ghosn, M.G. Jenkins, K.W. White, A.S. Kobayashi, and R.C. Bradt, "Elevated-Temperature Fracture Resistance of a Sintered  $\alpha$ -Silicon Carbide," *J. Am. Ceram. Soc.*, 72 [2] pp. 242–247, 1989.

**TABLE 2 Fracture Toughness of Hot-Pressed Silicon Nitride (NC 132) in MPa  $\sqrt{m}$** 

(n) = Number of test specimens tested  
 $\pm$  = 1 Standard Deviation  
 ? = quantity unknown

Precracked Beam (pb)	Surface Crack in Flexure (sc)	Chevron-Notch (vb)	Ref
...	4.59 $\pm$ 0.37 (107)	4.42 $\pm$ 0.14 (2)	<sup>A</sup>
4.67 $\pm$ 0.3 (7) Stable	4.64 $\pm$ 0.4 (5) <sup>B</sup>	...	<sup>C</sup>
4.50 $\pm$ 0.43 (3) Stable	...	4.85 $\pm$ ? (4)	<sup>D</sup>
4.54 $\pm$ 0.12 (7) Unstable	...	...	<sup>E</sup>
4.19 $\pm$ 0.19 (5) Stable	...	4.84 $\pm$ ? (4)	<sup>F</sup>
...	4.65 $\pm$ 0.10 (?) <sup>B</sup>	...	<sup>G</sup>
...	4.64 $\pm$ 0.25 (4) <sup>B</sup>	...	<sup>H</sup>
...	4.48 $\pm$ 0.07 (4) <sup>B</sup>		
	4.33 $\pm$ 0.37 (3) <sup>B</sup>		
4.59 $\pm$ 0.12 (11) <sup>I</sup> Valid <sup>J</sup>	4.55 $\pm$ 0.14 (14) <sup>I</sup> Valid <sup>J</sup>	4.60 $\pm$ 0.13 (8) <sup>I</sup> Valid <sup>J</sup>	<sup>K</sup>

<sup>A</sup>G.D. Quinn, J.J. Kübler, and R.J. Gettings, "Fracture Toughness of Advanced Ceramics by the Surface Crack in Flexure (SCF) Method: A VAMAS Round Robin," VAMAS Report # 17, National Institute of Standards and Technology, Gaithersburg, MD, June 1994.

<sup>B</sup>Annealed to remove indentation residual stresses. Note that although annealing to remove residual stresses is not allowed for the sc method in this standard, data are included here for illustrative purposes.

<sup>C</sup>V. Tikare and S.R. Choi, "Combined Mode I and Mode II Fracture of Monolithic Ceramics," *J. Am. Ceram. Soc.*, 76 [9], pp. 2265–2272, 1993.

<sup>D</sup>J.A. Salem, J.L. Shannon, Jr., and M.G. Jenkins, "Some Observations in Fracture Toughness and Fatigue Testing with Chevron-Notched Specimen," in *Chevron Notch Fracture Test Experience: Metals and Non-Metals*, ASTM STP 1172, eds. K.R. Brown and F.I. Baratta, ASTM, West Conshohocken, PA, pp 9–25, 1992.

<sup>E</sup>I. Bar-On, F.I. Baratta, and K. Cho, "Crack Stability and Its Effect on Fracture Toughness of Hot-Pressed Silicon Nitride Beam Specimens," *J. Am. Ceram. Soc.*, Vol 79 [9], pp. 2300–2308, 1996.

<sup>F</sup>R.T. Bubsey, J.L. Shannon, Jr., and D. Munz, "Development of Plane Strain Fracture Toughness Test for Ceramics Using Chevron Notched Specimens," in *Ceramics for High Performance Applications III, Reliability*, eds. E.M. Lenoe, R.N. Katz, and J.J. Burke, Plenum, NY, pp. 753–771, 1983.

<sup>G</sup>J.J. Petrovic, L.A. Jacobson, P.K. Talty, and A.K. Vasudevan, "Controlled Surface Flaws in Hot-Pressed Si<sub>3</sub>N<sub>4</sub>," *J. Am. Ceram. Soc.*, 58 [3–4], pp. 113–116, 1975.

<sup>H</sup>G.D. Quinn and J.B. Quinn, "Slow Crack Growth in Hot-Pressed Silicon Nitride," in *Fracture Mechanics of Ceramics*, Vol 6, eds. R.C. Bradt, A.G. Evans, D.P.H. Hasselman, F.F. Lange, Plenum, NY pp. 603–636, 1983.

<sup>I</sup>Single Billet C

<sup>J</sup>Valid tests per the validity requirements of 9.2 of this test method.

<sup>K</sup>G.D. Quinn, J.A. Salem, I. Bar-On, and M.G. Jenkins, "The New ASTM Fracture Toughness of Advanced Ceramics: PS070–97," *Ceramic Engineering and Science Proceedings*, Vol 19, No 3, pp. 565–578, 1998.

results are obtained with the three test methods in this standard when used on SRM 2100. As discussed in 1.4, 6.1 and 6.2,  $K_{Ipb}$ ,  $K_{Isc}$ , and  $K_{Ivb}$  values may differ from each other (for example, (15)). Nevertheless, a comparison of test results obtained by the three different methods is instructive. Such comparisons are shown in Tables 1 and 2. The experimental procedures used in the studies cited in Tables 1 and 2 varied

somewhat and were not always in accordance with this standard, although the data are presented here for illustrative purposes. Table 1 contains results for sintered silicon carbide, an advanced ceramic which is known to be insensitive to environmental effects in ambient laboratory conditions. This material is also known to have a fracture toughness independent of crack size (flat R-curve). Table 2 contains results for a

K <sub>Ipb</sub> DATA SHEET					
Material:	Form:		Processing Details:		
Test Specimen ID:	Test System:		Elastic Modulus (GPa):		
Date:	Test Machine Compliance (m/N):		Mean grain size (10 <sup>-6</sup> m):		
Test Particulars	Data	Test Method Section	Fracture Test	Data	Test Method Section
Ambient Environment		9.3, 9.9	Crack Length, a (mm)		A2.3.5
Relative Humidity (%RH)		9.9	Center, a <sub>0.50</sub> (mm)		A2.3.5, Fig. 4.
Temperature (°C)		9.9	Right, a <sub>0.75</sub> (mm)		A2.3.5, Fig. 4.
			Left, a <sub>0.25</sub> (mm)		A2.3.5, Fig. 4.
Test Specimen/Crack Plane Orientation		3.2.3	Normalized Crack Length, a/W		A2.3.5
			Final Crack Plane Angle (°)		A2.3.6, Fig. A2.4
Flexure Configuration (3- or 4-point)		7.4			
Outer span, S <sub>o</sub> (mm)		7.4	Test Rate (mm/s)		9.7, A2.3.4
Inner span, S <sub>i</sub> (mm)		7.4			
Test Specimen Dimensions			Test Record		A2.3.7, Fig. A2.5
B (mm)		A2.1.1, Figs. 4 & A2.1	Details		
W (mm)		A2.1.1, Figs. 4 & A2.1			
Precracking	Data	Test Method Section	Calculation of K <sub>Ipb</sub>	Data	Test Method Section
Notch Dimensions (if used)			Maximum Force, P <sub>max</sub> (N)		9.8.1
Notch Length (mm)		A2.1.2.4, Fig. A2.3	Coefficient for Stress Intensity Factor, g (a/W) or f (a/w)		A2.5.2, A2.5.3, A2.5.4
Notch Thickness (mm)		A2.1.2.4, Fig. A2.3			
			Fracture Toughness, K <sub>Ipb</sub> (MPa √m)		A2.5
Number of Indents (if used)		A2.3.1			
Indentation Load (N)		A2.3.1	Crack Stability at Fracture (unstable/stable)		A2.3.7, Fig. A2.5
Fixture groove width (mm)		A2.3.3, Fig. A2.2			
Precracking test rate		A2.3.2	Valid K <sub>Ipb</sub> (Y/N)		9.2, A2.3.5, A2.3.6, A2.3.7, A2.6

**Fig. 7 Reporting table for determination of fracture toughness,  $K_{Ibh}$**

**FIG. 7 Reporting Table for Determination of Fracture Toughness,  $K_{Ipb}$**

K <sub>Isc</sub> DATA SHEET			
Material:	Form:	Processing Details:	
Test Specimen ID:	Test System:	Elastic Modulus (GPa):	
Date:	Test Machine Compliance (m/N):	Mean grain size (10 <sup>-6</sup> m):	
Test Particulars	Data	Test Method Section	Fracture Test
Ambient Environment		9.3, 9.9	Crack Dimensions
Relative Humidity (%RH)		9.9	a (mm)
Temperature (°C)		9.9	c (mm)
Test Specimen/Crack Plane Orientation		3.2.3	Crack Details (valid crack?)
Flexure Configuration (4-point only)		7.4	Test Rate (N/s)
Outer span, S <sub>o</sub> (mm)		7.4	
Inner span, S <sub>i</sub> (mm)		7.4	Test Record
Test Specimen Dimensions			Stable Crack Extension (Y/N)
B (mm)		A3.1.1, Figs. 5 & A3.1	Fractography (SEM/Optical)
Initial (pre-polish) W (mm)		A3.3.2.2, Figs. 5 & A3.1	
Precracking	Data	Test Method Section	Calculation of K <sub>Isc</sub>
Indent Type			Maximum Force, P <sub>max</sub> (N)
(Knoop or Canted Vickers)		A3.3.1, X3	Coefficients for Stress Intensity Factor
Indent Diagonal, d (mm)		A3.3.2.1	Deepest, Y <sub>d</sub>
Indent Depth, h (mm)		A3.3.2.1	Surface, Y <sub>s</sub>
Post-polish W (mm)		A3.3.2.5, A3.3.2.9	Measured Fracture Toughness, K <sub>Isc</sub> (MPa √m)
Amount removed by polish or hand grinding (mm)		A3.3.2.5, Fig. A3.5	Apparent Fracture Toughness, K <sub>Isc</sub> * (MPa √m)
Indentation Force (N)		A3.3.1.2	Valid K <sub>Isc</sub> (Y/N)
			9.2, A3.5, A3.6

Figure 8 Reporting table for determination of fracture toughness, K<sub>Isc</sub>

FIG. 8 Reporting Table for Determination of Fracture Toughness, K<sub>Isc</sub>

K <sub>IVb</sub> DATA SHEET				
Material:	Form:	Processing Details:		
Test Specimen ID:	Test System:	Elastic Modulus (GPa):		
Date:	Test Machine Compliance (m/N):	Mean grain size (10 <sup>-6</sup> m):		
Test Particulars	Data	Test Method Section	Fracture Test	Test Method Section
Ambient Environment		9.3, 9.9	Chevron Notch Details	A4.3.1, Figs. 6 & A4.1
Relative Humidity (%RH)		9.9	a <sub>0</sub> (mm)	A4.3.1, Figs. 6 & A4.1
Temperature (°C)		9.9	a <sub>11</sub> (mm)	A4.3.1, Figs. 6 & A4.1
			a <sub>12</sub> (mm)	A4.3.1, Figs. 6 & A4.1
Test Specimen/Crack Plane Orientation		3.2.3	Notch thickness, t (mm)	A4.4.2, Fig. A4.1
			Notch thickness <0.150 mm at root radius (Y/N)	A4.1.3, A4.3.4
Flexure Configuration (3- or 4-point)		7.4	Chevron tip within 0.02 B of specimen center (Y/N)	A4.1.3, A4.3.4
Outer span, S <sub>o</sub> (mm)		7.4		
Inner span, S <sub>i</sub> (mm)		7.4	Test Rate (mm/s)	9.7, A4.3.3
Test Specimen Dimensions				
B (mm)		A4.1, Figs. 6 & A4.1	Test Record	A4.3.6, Fig. A4.3
W (mm)		A4.1, Figs. 6 & A4.1	Details (stable/unstable)	
Precracking (if used)	Data	Test Method Section	Calculation of K <sub>IVb</sub>	Test Method Section
Chevron Notch Tip			Maximum Relevant Force, P <sub>max</sub> (N)	9.8.2, Fig. A4.3
in Compression (Y/N)		A4.4.1	Coefficient for Stress Intensity Factor, Y* <sub>min</sub>	A4.5.1, A4.5.2, A4.5.3, A4.5.4
			Fracture Toughness, K <sub>IVb</sub> (MPa √m)	A4.5.1
Maximum Compressive Force (N) (if applicable)		A4.4.1	Crack Stability at Fracture (Y/N)	A4.3.6, Fig. A4.3
Number of Load Cycles		A4.4.1	Valid K <sub>IVb</sub> (Y/N)	9.2, A4.3.5, A4.3.6, A4.6

Figure 9 Reporting table for determination of fracture toughness, K<sub>IVb</sub>

FIG. 9 Reporting Table for Determination of Fracture Toughness, K<sub>IVb</sub>



hot-pressed silicon nitride which has little or no dependence of fracture toughness on crack size and which also usually had negligible sensitivity to environmental effects in ambient laboratory conditions. The hot-pressed silicon nitride results are notably consistent. Some of the variability is due to differences in fracture toughness between billets of this material (See footnotes *I* and *K* in Table 2). The results of the last

line in Table 2 were generated from a single billet identified as “C.”

## 12. Keywords

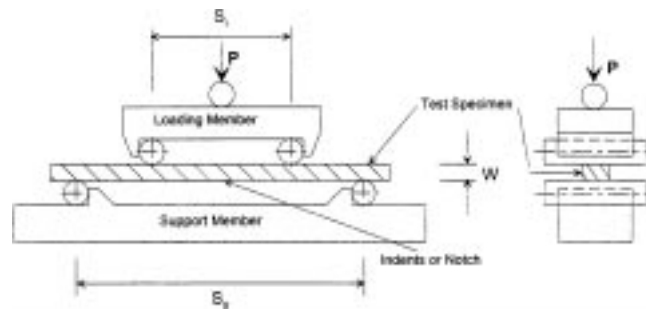
12.1 advanced ceramics; chevron notch; fracture toughness; precracked beam; surface crack in flexure

## ANNEXES

### (Mandatory Information)

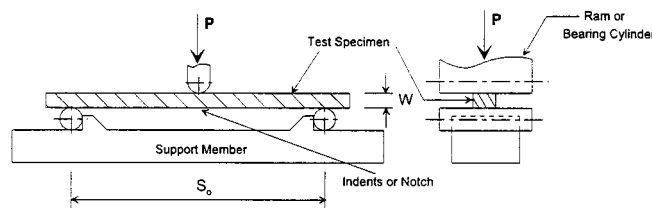
#### A1. SUGGESTED TEST FIXTURE SCHEMATICS

A1.1 See Fig. A1.1 and Fig. A1.2.



NOTE 1—All Rollers are 4.5 mm in diameter.

FIG. A1.1 Four-point test fixture schematic which illustrates the general requirements for a semi-articulating fixture.



NOTE 1—All Rollers are 4.5 mm in diameter.

FIG. A1.2 Three-point test fixture schematic which illustrates the general requirements of the test fixture.

#### A2. SPECIAL REQUIREMENTS FOR THE PRECRACKED BEAM METHOD

##### A2.1 Test Specimen

A2.1.1 *Test Specimen Size*—The test specimen shall be 3 by 4 mm in cross section with the tolerances shown in Fig. A2.1. The test specimen may or may not contain a saw-cut notch. For both four-point and three-point flexure tests the length shall be at least 20 mm but not more than 50 mm.

A2.1.1.1 Test specimens of larger cross section can be tested as long as the proportions given in Fig. A2.1 are maintained.

A2.1.1.2 The stability (that is, the tendency to obtain stable crack extension) of the test set up is affected not only by the test system compliance (see Note 7) but also by the test specimen dimensions, the  $S_0/W$  ratio, and the elastic modulus

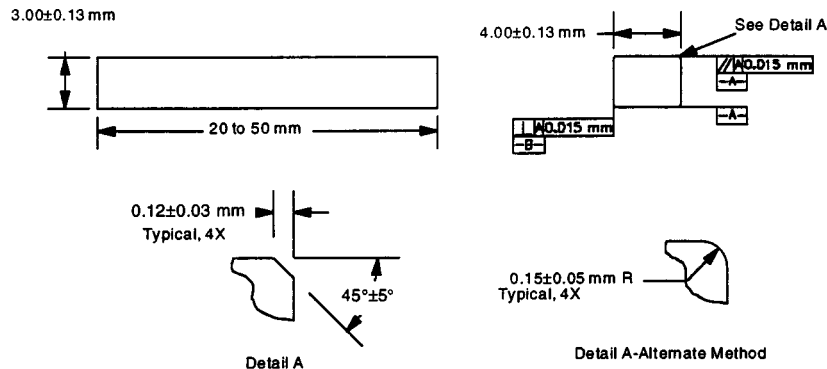


FIG. A2.1 Dimensions of Rectangular Beam

of the material (8, 9).

**A2.1.2 Test Specimen Preparation**—Test specimens prepared in accordance with the Procedure of Test Method C 1161, test specimen Type B, are suitable as summarized in the following paragraphs, A2.1.2.1-A2.1.2.3. Any alternative procedure that is deemed more efficient may be utilized provided that unwanted machining damage and residual stresses are minimized. Report any alternative test specimen preparation procedure in the test report.

**A2.1.2.1** All grinding shall be done with an ample supply of appropriate filtered coolant to keep workpiece and wheel constantly flooded and particles flushed. Grinding shall be in at least two stages, ranging from coarse to fine rates of material removal. All machining shall be in the surface grinding mode parallel to the test specimen long axis. No Blanchard or rotary grinding shall be used. The stock removal rate shall not exceed 0.02 mm per pass to the last 0.06 mm per face.

**NOTE A2.1**—These conditions are intended to minimize machining damage or surface residual stresses. As the grinding method of Test Method C 1161 is well established and economical, it is recommended.

**A2.1.2.2** Perform finish grinding with a diamond-grit wheel of 320 grit or finer. No less than 0.06 mm per face shall be removed during the final finishing phase, and at a rate of not more than 0.002 mm per pass.

**A2.1.2.3** The two end faces need not be precision machined. The four long edges shall be chamfered at 45° a distance of 0.12 ± 0.03 mm, or alternatively, they may be rounded with a radius of 0.15 ± 0.05 mm as shown in Fig. A2.1. Edge finishing shall be comparable to that applied to the test specimen surfaces. In particular, the direction of the machining shall be parallel to the test specimen long axis.

**A2.1.2.4** The notch, if used, should be made in the 3-mm face, should be less than 0.10 mm in thickness, and should have a length of  $0.12 \leq a/W \leq 0.30$ .

**A2.1.3** It is recommended that at least ten test specimens be prepared. This will provide test specimens for practice tests to determine the best precracking parameters. It will also provide make-up test specimens for unsuccessful or invalid tests so as to meet the requirements of 9.1 and 9.2.

## A2.2 Apparatus

**A2.2.1 General**—This fracture test is conducted in either three- or four-point flexure. However, the configuration used for precracking is different from that used for the actual

fracture test. A displacement measurement (or alternative) is required.

**A2.2.2 Precracking Fixture**—A compression fixture is used to create a precrack from an indentation crack or from a sawed notch. The fixture consists of a square support lower plate with a center groove (which is bridged by the test specimen) and a top pusher plate with a bonded pusher plate insert (for example, silicon nitride). The lengths of both plates ( $L_1$  in Fig. A2.2) are equal to each other and are less than or equal to 18 mm. The surfaces that contact the test specimen are of a material with an elastic modulus greater than 196 GPa. The support plate can have several grooves ( $L_2$  in Fig. A2.2) ranging from 2 to 6 mm in width. Alternatively, several parts, each with a different groove width can be used. A fixture design is shown in Fig. A2.2. The support and pusher plates shall be parallel within 0.01 mm. Alternatively, a self-aligning fixture can be used.

**A2.2.3 Fracture Test Fixture**—The general principles of the four- and three-point test fixture are detailed in 7.4 and illustrated in Fig. A1.1 and Fig. A1.2, respectively. For three-point flexure, choose the outer support span such that  $4 \leq \frac{S_o}{W} \leq 10$ .

## A2.3 Procedure

**A2.3.1 Preparation of Crack Starter**—Either the machined notch (Fig. A2.3a), a Vickers indent, or a series of Vickers indents (Fig. A2.3b) act as the crack starter. For a test specimen without a notch, create a Vickers indent in the middle of the surface of the 3-mm face (Fig. A2.3b). Additional indents can

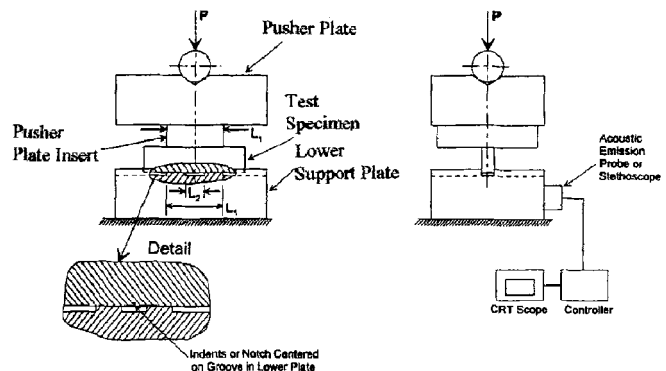
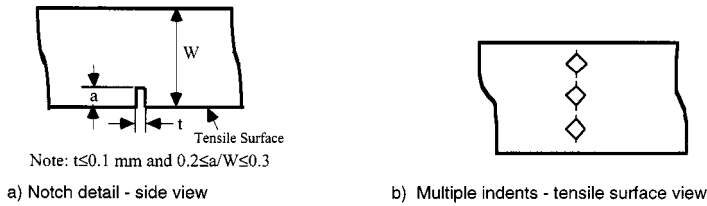


FIG. A2.2 Suggestion for Bridge Compression Fixture (16)

FIG. A2.2 Suggestion for Bridge Compression Fixture (16)



**FIG. A2.3 Precracked Beam Precracking Arrangement**

be placed on both sides of the first indent, aligned in the same plane and perpendicular to the longitudinal axis of the test specimen, as shown in Fig. A2.3b. One of the diagonals of each of the indents shall be aligned parallel to the test specimen length. The indent force shall not exceed 100 N. While an indentation crack is physically necessary for subsequent generation of a pop-in crack, cracks emanating from the corners of the indentation may or may not be visible depending on the characteristics and finish of the test material. Alternatively, a Knoop indent may also be used as a crack starter in which case, the long axis of the indent shall be perpendicular to the longitudinal axis of the test specimen. If, for a particular test material, a pop-in crack does not form from the indent produced by the 100 N indentation, then it may be necessary to first form a saw notch as a crack starter.

**NOTE A2.2**—The 100 N indent force limit is intended to minimize potential residual tensile stresses which could influence the fracture results. If residual stresses from the indentation are suspected to have affected the fracture results, the indentations may be removed by polishing, hand grinding or grinding after the precrack has been formed (A2.3.2). Annealing may be used provided that the crack tip is not blunted nor the crack tip/planes healed.

**A2.3.2 Formation of Precrack**—Thoroughly clean the test specimen and contacting faces of the compression fixture. Place the test specimen in the compression fixture with the surface containing the notch or indent(s) over the groove and the notch or indent(s) centered between the edges of the groove. Load the test specimen in the compression fixture at rates up to 1000 N/s until a distinct pop-in sound is heard and/or until a pop-in precrack is seen. At high force rates it may not be possible to discern the force drop in the applied force-displacement curve as discussed in 3.2.10. A stethoscope or other acoustic transducer can also be used to detect the pop-in sound. A traveling microscope is also recommended to view the pop-in crack as the pop-in sound is not always discernible. In some materials it is difficult to see a precrack on the side of the test specimens. Lapping of the side surface or use of a dye penetrant, or both, (see A2.3.2.1) can help delineate the crack. Stop loading immediately after pop-in. Measure the pop-in crack on both side surfaces. The precrack length should be between 0.35 and 0.60W.

**NOTE A2.3**—For materials with a rising R-curve the  $K_{Ipb}$  value might be artificially high if the precrack is not stopped immediately after pop-in. The force rate during pop-in may influence the crack/microstructure interaction and may affect the result.

**NOTE A2.4—Caution:** Use care not to overload the testing machine or load cell.

**A2.3.2.1** A drop of the dye penetrant can be placed on indentations or saw notch. Upon formation of the precrack, the penetrant will be drawn into the crack and will show on the

side surface of the test specimen upon unloading.

**NOTE A2.5—Caution:** Use care to ensure that dye penetrants are dry (for example, by heating) or do not promote corrosion or slow crack growth, prior to fracture testing to preclude undesired slow crack growth or undesired crack face bonding.

**A2.3.3 Choice of Groove**—The pop-in precrack length is a result of the selected indent force and groove size of the compression fixture. These two parameters need to be determined by trial and error. It has been shown that the pop-in precrack length decreases with increasing indent force and with decreasing groove (span) size (16, 17).

**A2.3.4 Fracture Test**—Insert the test specimen into the flexure fixture. Align the tip of the crack with the centerline of the middle roller in the three-point flexure fixture within 0.5 mm or within 1.0 mm of the midpoint between the two inner rollers,  $S_i$ , of the four-point flexure fixture. Test the test specimen in actuator displacement (stroke) control at a rate in agreement with 9.7. Record applied force versus displacement or alternative (for example, actuator displacement (stroke), load-point displacement, displacement of the test specimen at the crack plane), back-face strain (10) or time.

**NOTE A2.6**—Generally, actuator displacement (stroke) rates of 0.0005 to 0.01 mm/s for test specimens with a  $3 \times 4$  mm cross section provide stress intensity factor rates in accordance with 9.7.

**NOTE A2.7**—Actuator displacement (stroke) may not be as sensitive to changes of fracture behavior in the test specimen as measurements taken on the test specimen itself, such as back-face strain, load-point displacement, or displacement at the crack plane (10).

**NOTE A2.8**—The requirement for centering the test specimen is much easier to fulfill for a four-point flexure test (18). A three-point flexure test requires that the crack plane be centered accurately in the test fixture.

**A2.3.5 Post Test Measurements**—Fractographically measure the crack length after fracture to the nearest 1 % of W at a magnification greater than or equal to  $20 \times$  at the following three positions: at the center of the precrack front and midway between the center of the crack front and the end of the crack front on each surface of the test specimen (Fig. 4). Use the average of these three measurements to calculate  $K_{Ipb}$ . The difference between the average crack length and the minimum precrack length measurement shall be less than 10 %. The average precrack length, a, shall be within the following range:  $0.35W \leq a \leq 0.60W$ . If the crack was started from a notch, the precrack length, a, shall also be longer than the sum of the notch length and one notch thickness.

**A2.3.6** The plane of the final crack measured from the tip of the precrack shall be parallel to both the test specimen dimensions B and W within  $\pm 5^\circ$  for three-point flexure and within  $\pm 10^\circ$  for four-point flexure, as illustrated in Fig. A2.4.

**A2.3.7** Inspect the applied force-displacement curves. As illustrated in Fig. A2.5, the applied force-displacement curves can indicate a) unstable crack extension (Fig. A2.5a), pop-in (or crack jump) behavior (stable) (Fig. A2.5b), or smooth stable crack extension (Fig. A2.5c). Unstable crack extension may give greater fracture toughness values than those from tests with stable crack extension.

**A2.3.8** If there is evidence of environmentally-assisted slow crack growth then it is advisable to run additional tests in an inert environment. Alternatively, additional tests may be done in laboratory ambient conditions at faster or slower test rates

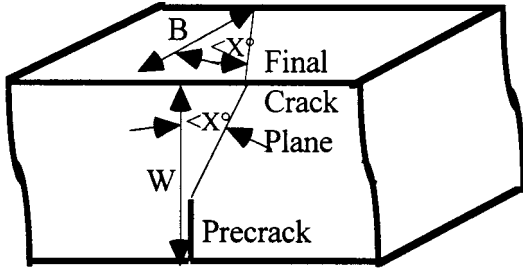


FIG. A2.4 Illustration of Angular Allowance of Final Crack Plane Where  $X^\circ$  is  $5^\circ$  for Three-Point Flexure and  $10^\circ$  for Four-Point Flexure

than those specified in this standard in order to determine the sensitivity to test rates. Testing rates that differ by two to three orders of magnitude or greater than those specified are recommended. (See 9.3.)

#### A2.4 Recommendations

A2.4.1 Pre-cracked beam tests can be either stable or unstable. Unstable tests may result in greater fracture toughness values than those from tests with stable crack extension (8, 9). If stable crack extension cannot be obtained with four-point flexure, it may be possible to obtain stable crack extension by using a three-point flexure configuration in a stiff test setup.

A2.4.2 Nonlinearity of the initial part of the applied force-displacement curve (sometimes called “windup”) is usually an artifact of the test setup and may not be indicative of material behavior. This type of nonlinearity does not contribute directly to instability unless such nonlinearity extends to the region of maximum force.

#### A2.5 Calculation

A2.5.1 Calculate the fracture toughness,  $K_{Ipb}$ , for each test specimen and test configuration.

A2.5.2 For three-point flexure with  $\frac{S_o}{W} = 4$ ,  $0.35 \leq \frac{a}{W} \leq 0.60$  and a maximum error of 2 % (19) (see also Note A2.1):

$$K_{Ipb} = g \left[ \frac{P_{max} S_o 10^{-6}}{B W^{3/2}} \right] \left[ \frac{3[a/W]^{1/2}}{2[1-a/W]^{3/2}} \right] \quad (A2.1)$$

where:

$$g = g(a/W) = \frac{1.99 - [a/W][1 - a/W][2.15 - 3.93[a/W] + 2.7[a/W]^2]}{1 + 2[a/W]} \quad (A2.2)$$

Eq A2.1 and Eq A2.2 have also been used for  $\frac{S_o}{W} = 5$  (20)

with maximum errors of 1.5 % for  $0.35 \leq \frac{a}{W} \leq 0.60$ .

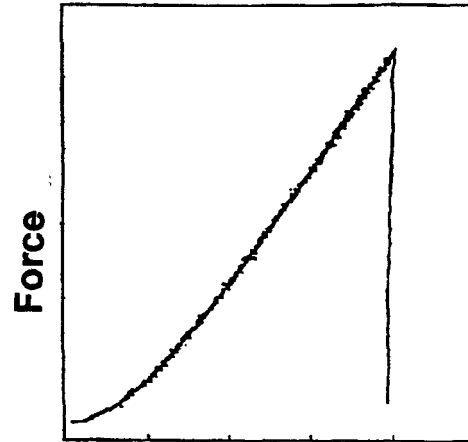
*Example*—For  $W = 4.00 \text{ mm} = 4.00 \times 10^{-3} \text{ m}$ ,  $a_o = 2.00 \text{ mm} = 2.00 \times 10^{-3} \text{ m}$  and  $S_o = 16.0 \text{ mm} = 16.0 \times 10^{-3} \text{ m}$  then  $a/W = 0.50$ ,  $S_o/W = 4.0$ ,  $g = 0.8875$ .

A2.5.3 For three-point flexure with  $5 \leq \frac{S_o}{W} \leq 10$ ,  $0.35 \leq \frac{a}{W} \leq 0.60$  and a maximum error of 1.5 % (9):

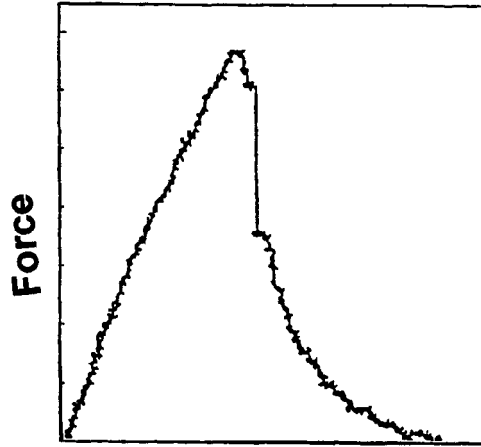
$$K_{Ipb} = g \left[ \frac{P_{max} S_o 10^{-6}}{B W^{3/2}} \right] \left[ \frac{3[a/W]^{1/2}}{2[1-a/W]^{3/2}} \right] \quad (A2.3)$$

where:

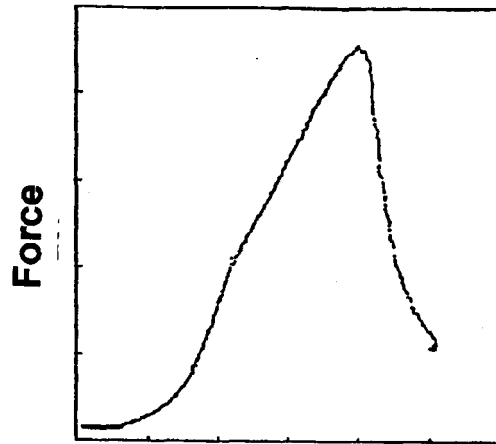
$$g = g(a/W) = A_0 + A_1(a/W) + A_2(a/W)^2 + A_3(a/W)^3 + A_4(a/W)^4 + A_5(a/W)^5 \quad (A2.4)$$



a) Unstable crack extension



b) Pop-in Behavior - stable



c) Stable Crack Extension

FIG. A2.5 Load Displacement Diagrams from Pre-cracked Beam Tests



where coefficients for  $g$  are shown in Table A2.1

**Example**—For  $W = 4.00 \text{ mm} = 4.00 \times 10^{-3} \text{ m}$ ,  $a_o = 2.00 \text{ mm} = 2.00 \times 10^{-3} \text{ m}$  and  $S_o = 40.0 \text{ mm} = 40.0 \times 10^{-3} \text{ m}$  then  $a/W = 0.50$ ,  $S_o/W = 10.0$ ,  $g = 0.9166$ .

A2.5.4 For four-point flexure with  $0.35 \leq \frac{a}{W} \leq 0.60$  and a maximum error of 2 % (21):

$$K_{Ipb} = f \left[ \frac{P_{\max}[S_o - S_i]10^{-6}}{BW^{3/2}} \right] \left[ \frac{3[a/W]^{1/2}}{2[1 - a/W]^{3/2}} \right] \quad (\text{A2.5})$$

where:

$$\begin{aligned} f &= f(a/W) \\ &= 1.9887 - 1.326[a/W] \\ &\quad - \frac{\{3.49 - 0.68[a/W] + 1.35[a/W]^2\}[a/W]\{1 - [a/W]\}}{\{1 + [a/W]\}^2} \end{aligned} \quad (\text{A2.6})$$

**Example**—For  $W = 4.00 \text{ mm} = 4.00 \times 10^{-3} \text{ m}$ ,  $a_o = 2.00 \text{ mm} = 2.00 \times 10^{-3} \text{ m}$ ,  $S_o = 40.0 \text{ mm} = 40.0 \times 10^{-3} \text{ m}$  and  $S_i = 20.0 \text{ mm} = 20.0 \times 10^{-3} \text{ m}$  then  $a/W = 0.50$ ,  $f = 0.9382$ .

where:

- $K_{Ipb}$  = fracture toughness ( $\text{MPa} \sqrt{\text{m}}$ ),
- $f = f(a/W)$  = function of the ratio  $a/W$  for four-point flexure,
- $g = g(a/W)$  = function of the ratio  $a/W$  for three-point flexure,
- $P_{\max}$  = maximum force as determined in 9.8.1 (N),
- $S_o$  = outer span (m),
- $S_i$  = inner span (m),
- $B$  = side to side dimension of the test specimen perpendicular to the crack length (depth) as shown in Fig. 4 (m),
- $W$  = top to bottom dimension of the test specimen parallel to the crack length (depth) as shown in Fig. 4 (m), and
- $a$  = crack length as determined in A2.3.5 (m).

## A2.6 Valid Test

A2.6.1 A valid pb test shall meet the following requirements in addition to the general requirements of these test methods (9.2):

A2.6.1.1 Test specimen size (A2.1.1) shall be 3 by 4 mm with tolerances as shown in Fig. A2.1 and the length shall be at least 20 mm but not more than 50 mm unless test specimens of larger cross section are used as long as the proportions given in Fig. A2.1 are maintained.

A2.6.1.2 Test specimen preparation (A2.1.2) shall conform to the procedures of A2.1.2.

A2.6.1.3 Crack starter (A2.3.1) introduced from Vickers indent shall be produced at an indent force  $\leq 100 \text{ N}$  and one of the diagonals of each of the indents shall be aligned parallel to the test specimen length.

A2.6.1.4 Pop-in precrack (A2.2.2 and A2.3.2) shall be introduced using a grooved compression fixture.

A2.6.1.5 Crack length (A2.3.5): difference between average crack length and minimum precrack length shall be less than 10 % and average precrack length shall be  $0.35W < a < 0.6W$ .

A2.6.1.6 Plane of final crack (A2.3.6) shall be parallel to both the test specimen dimensions  $B$  and  $W$  within  $\pm 5^\circ$  for three-point flexure and  $\pm 10^\circ$  for four-point flexure.

## A2.7 Reporting Requirements

A2.7.1 In addition to the general reporting requirements of 10.1, 10.2 and 10.3 report the following for the pb method.

A2.7.1.1 Mean crack length as measured in A2.3.5 (mm),

A2.7.1.2 Each applied force-displacement (time or strain) diagram with a statement about stability (see A2.3.7 and Fig. A2.5), and

A2.7.1.3 Precracking details, such as the number of indents, indentation force and the force rate during pop-in.

## A2.8 Precision

A2.8.1 Results from an eighteen-laboratory, international round robin conducted under the auspices of the Versailles Advanced Materials and Standards (VAMAS) can be used to estimate the precision of the pb method (13, 22, 23). A gas pressure sintered silicon nitride was tested by procedures that were similar to those prescribed in this Test Method. An important exception was that specific actuator displacement (stroke) rates were prescribed, rather than stress intensity factor rates. Two actuator displacement (stroke) rates, 0.0166 mm/s and 0.0000833 mm/s were prescribed. This permitted an assessment of whether time-dependent environmental effects were present. Ten test specimens were tested at each test rate by each laboratory. A variety of test fixtures and test rates were used for precracking. Machine compliance was not prescribed or reported in the project, but it is likely that most crack extensions were unstable.

A2.8.2 The VAMAS round robin results were analyzed in accordance with Practices E 177 and E 691. The results are given in Table A2.2.

A2.8.3 The VAMAS round robin also included pb testing on a zirconia-alumina composite material. Environmentally-assisted crack growth and possible rising R-curve behavior caused complications in interpretation of the results as discussed in Ref. (13).

A2.8.4 A slight loss of accuracy and precision may result from the use of very short 3-point spans as discussed in

TABLE A2.1 Coefficients for the Polynomial  $g(a/W)$  for Three-point Flexure

	$S_o/W$				
	5	6	7	8	10
$A_o$	1.9109	1.9230	1.9322	1.9381	1.9472
$A_1$	-5.1552	-5.1389	-5.1007	-5.0947	-5.0247
$A_2$	12.6880	12.6194	12.3621	12.3861	11.8954
$A_3$	-19.5736	-19.5510	-19.0071	-19.2142	-18.0635
$A_4$	15.9377	15.9841	15.4677	15.7747	14.5986
$A_5$	-5.1454	-5.1736	-4.9913	-5.1270	-4.6896

TABLE A2.2 Precracked Beam Results from VAMAS Round Robin for Gas-Pressure Sintered Silicon Nitride (13,22,23)

Test Rates mm/s <sup>A</sup>	Number of Laboratories <sup>B</sup>	Overall Mean MPa√m	Repeatability (Within-Laboratory)			Reproducibility (Between-Laboratories)		
			Std Dev MPa√m	95 %limit MPa√m	COV <sup>C</sup> %	Std Dev MPa√m	95 %limit MPa√m	COV <sup>C</sup> %
0.0166 or (0.0083)	16	5.77	0.26	0.72	4.5	0.51	1.42	8.8
0.000083 or (0.000167, 0.000042)	12	5.60	0.26	0.73	4.7	0.40	1.11	7.1

<sup>A</sup>Numbers in parentheses show alternative test rates that some laboratories used rather than the specified rates.

<sup>B</sup>At each test rate the results from one laboratory were deleted, due to high within-laboratory (repeatability) scatter.

<sup>C</sup>Coefficient of variation.

Reference 12. The precrack ( ) and middle-roller fixture alignment (Note Note 12 and 9.6.1) tolerances specified in this

standard lead to a maximum possible 3 % error un  $K_{I, pb}$ .

### A3. SPECIAL REQUIREMENTS FOR THE SURFACE-CRACK IN FLEXURE METHOD

#### A3.1 Test Specimen

**A3.1.1 Test Specimen Size**—The test specimen shall be 3 X 4 mm in cross section with the tolerances shown in Fig. A3.1. The length shall be 45 to 50 mm. Half length test specimens with cross-section dimensions of 3 X 4 mm and lengths of 25 mm or greater may also be used.

**A3.1.2 Test Specimen Preparation**—Test specimens prepared in accordance with the Procedure of Test Method C 1161, test specimen Type B, are suitable as summarized in the A3.1.2.1-A3.1.2.4. Any alternative procedure that is deemed more efficient may be utilized provided that unwanted machining damage and residual stresses are minimized. Report any alternative test specimen preparation procedure in the test report.

**A3.1.2.1** All grinding shall be done with an ample supply of appropriate filtered coolant to keep workpiece and wheel constantly flooded and particles flushed. Grinding shall be in at least two stages, ranging from coarse to fine rates of material removal. All machining shall be in the surface grinding mode parallel to the test specimen long axis. No Blanchard or rotary grinding shall be used. The stock removal rate shall not exceed 0.02 mm per pass to the last 0.06 mm per face.

**NOTE A3.1**—These conditions are intended to minimize machining damage or surface residual stresses which can strongly affect tests using sc test specimens. As the grinding method of Test Method C 1161 is well established and economical, it is recommended.

**A3.1.2.2** For all surfaces except that to be indented perform finish grinding with a diamond-grit wheel of 320 grit or finer.

No less than 0.06 mm per face shall be removed during the final finishing phase, and at a rate of not more than 0.002 mm per pass.

**A3.1.2.3** For the surface to be indented (either the 3- or 4-mm dimension), a diamond-grit wheel (320 to 500 grit) shall be used to remove the last 0.04 mm at a rate of not more than 0.002 mm per pass. Polish, lap or fine grind this face to provide a flat, smooth surface for the surface crack. It can alternatively be ground with a 600-grit or finer wheel, provided that residual stresses are not introduced.

**NOTE A3.2**—The indent can be placed in either the 3- or 4-mm dimension surface of the beam. The surface need not have an optical quality finish. It need only be flat such that the indent is not affected by machining striations and marks.

**A3.1.2.4** The two end faces need not be precision machined. The four long edges shall be chamfered at 45° a distance of  $0.12 \pm 0.03$  mm, or alternatively, they may be rounded with a radius of  $0.15 \pm 0.05$  mm as shown in Fig. A3.1. Edge finishing shall be comparable to that applied to the test specimen surfaces. In particular, the direction of the machining shall be parallel to the test specimen long axis.

**A3.1.3** It is recommended that at least ten and preferably twenty test specimens be prepared. This will provide test specimens for practice tests to determine the best indentation force. It will also provide make up test specimens for unsuccessful or invalid tests so as to meet the requirements of 9.1 and 9.2.

#### A3.2 Apparatus

**A3.2.1 General**—Conduct this test in four-point flexure. A displacement measurement is not required.

**A3.2.2 Fracture Test Fixture**—The general principles of the four-point test fixture are detailed in 7.4 and illustrated in A1.1.

#### A3.3 Procedure

##### A3.3.1 Precracking—Standard Procedure:

**A3.3.1.1** Use a Knoop indenter to indent the middle of the polished surface of the test specimen. Orient the long axis of the indent at right angles (within 2°) to the long axis of the test specimen as shown in Fig. A3.2. Tilt the test specimen ¼° to

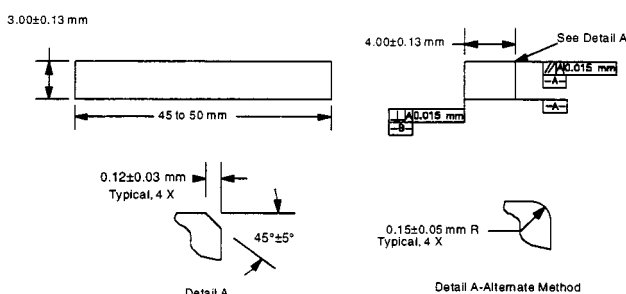


FIG. A3.1 Dimensions of Rectangular Beam

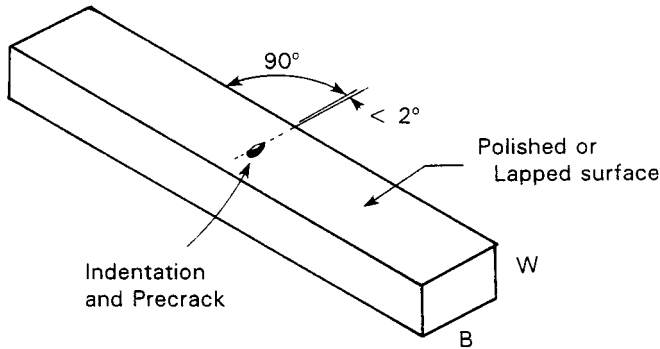


FIG. A3.2 Surface-Crack in Flexure (sc) Test Specimen

$\frac{1}{2}^\circ$  as shown in Fig. A3.3. Use a full-force dwell time of 15 s or more during the indentation cycle. A schematic of a resulting precrack is shown in Fig. 5 and Fig. A3.3.

NOTE A3.3—The  $\frac{1}{4}^\circ$  to  $\frac{1}{2}^\circ$  tilt is intended to make the precrack easier to discern during measurement of precrack size after fracture. The  $\frac{1}{2}^\circ$  test specimen tilt will lead to precrack tilts that range from 0 to  $5^\circ$ . The effect of this tilt upon the measured fracture toughness is insignificant as discussed in Ref. (14).

NOTE A3.4—In some instances such as with zirconia, indentation times longer than 15 s may be helpful.

A3.3.1.2 The indentation force,  $F$ , used may have to be determined for each different class of material by the use of a few trial test specimens. The force must be great enough to create a crack that is greater than the naturally-occurring flaws in the material, but not too great relative to the test specimen cross section size, nor so great that extreme impact damage occurs. Indentation forces of approximately 10 to 20 N are suitable for very brittle ceramics, 25 to 50 N for medium “tough” ceramics, and 50 to 100 N for very “tough” ceramics.

NOTE A3.5—This indentation procedure to create a surface crack will

not be successful on very soft (low hardness) or porous ceramics since a precrack will not form under the Knoop indent. The process may not work on very “tough” ceramics either, since they will be resistant to the formation of cracks, or the crack which does form will be very small and will likely be removed during the subsequent material removal step (see A3.3.2) to remove the residual stress and damage zone.

NOTE A3.6—An indentation force of 30 N may be suitable for most glasses.

### A3.3.2 Removal of Indented Zone:

A3.3.2.1 Measure the length of the long diagonal,  $d$ , of the Knoop impression to within 0.005 mm.

NOTE A3.7—This measurement need not be done to the precision required for hardness measurements. If Knoop hardness is to be reported, greater care should be exercised in making the diagonal size measurement and in the preparation of the initial test specimen surface.

Calculate the approximate depth,  $h$ , of the Knoop impression as follows:

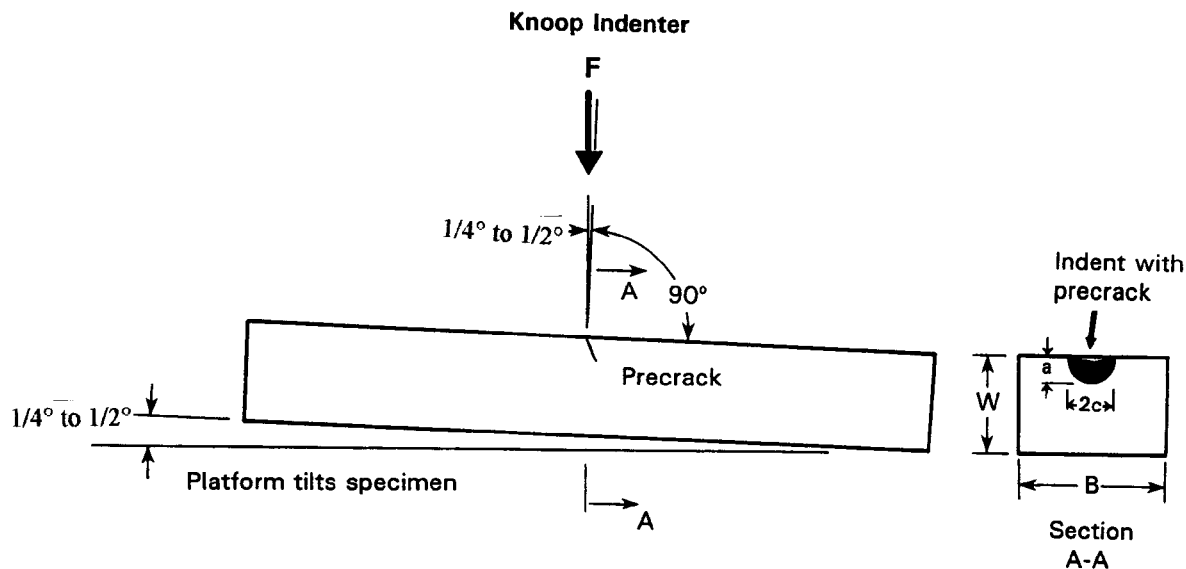
$$h = d/30 \quad (\text{A3.1})$$

A3.3.2.2 Measure the initial (pre-polishing) test specimen dimension,  $W$ , at the indent location to within 0.002 mm. A hand-held micrometer with a vernier graduation is suitable.

A3.3.2.3 Mark the side of the test specimen with a pencil-drawn arrow in order to indicate the surface with the precrack and its approximate location.

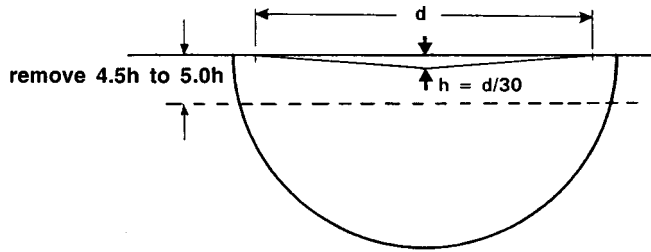
A3.3.2.4 Remove the residual stress damage zone by mild grinding, hand grinding, or hand polishing with abrasive papers.

A3.3.2.5 Hand lapping or grinding may be done wet or dry, with the type of procedure reported. Remove an amount of material that is approximately equal to 4.5 to 5.0  $h$  as shown in Fig. A3.4. If there is evidence that this material removal has not eliminated deep lateral cracks, then additional material should be removed. Remnant lateral cracks are more apt to be a problem with brittle materials (for example,  $K_{Isc} < 3.0 \text{ MPa m}$ ).



NOTE 1—The indent and precrack sizes are exaggerated for clarity.

FIG. A3.3 The Test Specimen may be Indented at a  $\frac{1}{2}^\circ$  Tilt in Order to Enhance the Chances of Detecting the Precrack on the Fractographic Surface During Subsequent Fracture Analysis. The indentation may be introduced in either the narrow 3-mm face or the wide 4-mm face.



NOTE 1—Remove 4.5h to 5.0h from the test specimen surface in order to remove the indent and damage zone.

**FIG. A3.4 The Precrack Extends Below the Knoop Hardness Impression, which has Depth,  $h$**

The material removal process shall not induce residual stresses or excessive machining damage in the test specimen surface. Remove the last 0.005 mm with a finer grit (220 to 280 grit) paper with less pressure, so as to minimize polishing damage. Check the test specimen dimension,  $W$ , frequently during this process. In particular, the evenness of  $W$  should be monitored. A hand micrometer should be used to check  $W$  at several locations across the specimen width  $B$  in the vicinity of the indentation. Use a hand micrometer with a resolution of 0.0025 mm or better.

NOTE A3.8—Experience has demonstrated that hand grinding the test specimen with 180 to 220 grit silicon carbide paper can remove the required amount in 1 to 5 min per test specimen for many ceramics. Faster removal rates occur when hand grinding dry. Finer-grit (320 to 400 grit) papers are recommended for glasses for both rough- and fine- grinding steps. Diamond impregnated abrasive disks with 30  $\mu$ m or finer abrasive may also be used.

NOTE A3.9—Hand lapping or grinding may make the surface uneven or not parallel to the opposite test specimen face. This can cause misalignments during subsequent testing on test fixtures. If the polished face cannot be maintained parallel to the opposite face within  $\pm 0.015$  mm, then fully-articulating fixtures should be used for flexure testing in accordance with 7.4.3. A slight rounding of the edges of the test specimen from hand grinding is usually inconsequential. In a given test specimen, regularly change the orientation of the surface being polished to the lapping disk during material removal steps to minimize unevenness.

NOTE A3.10—**Warning:** Fine ceramic powders or fragments may be created if the lapping or hand grinding is done dry. This can create an inhalation hazard if the ceramic contains silica or fine whiskers. Masks or respirators should be used, or the removal should be done wet.

NOTE A3.11—The removal of 4.5 to 5.0 h will eliminate the residual stress damage zone under the impression, and usually will leave a precrack shape that has the highest stress intensity factor at the deepest part of the precrack periphery. The location of the maximum stress intensity can be controlled by the amount of material removed. The initial precrack under the Knoop indent is roughly semicircular and  $Y_{max}$  is at the surface. As material is removed, the precrack becomes more semi-elliptical in shape (or like a section of a circle) and  $Y_{max}$  will shift to the deepest part of the precrack. If too much material is removed, the remaining precrack will be too small and fracture will not occur from the precrack. In such cases smaller amounts should be removed, provided that no less than 3 h is removed. If this step is not adequate to ensure fracture from the precrack, then a greater indent force or the alternative procedure described in Appendix X3 may be used.

A3.3.2.6 Surface grinding with diamond wheels is also permitted as a means to remove the indent and residual stress damage zone, but it is much more difficult to ensure that the correct amount of material has been removed from each test

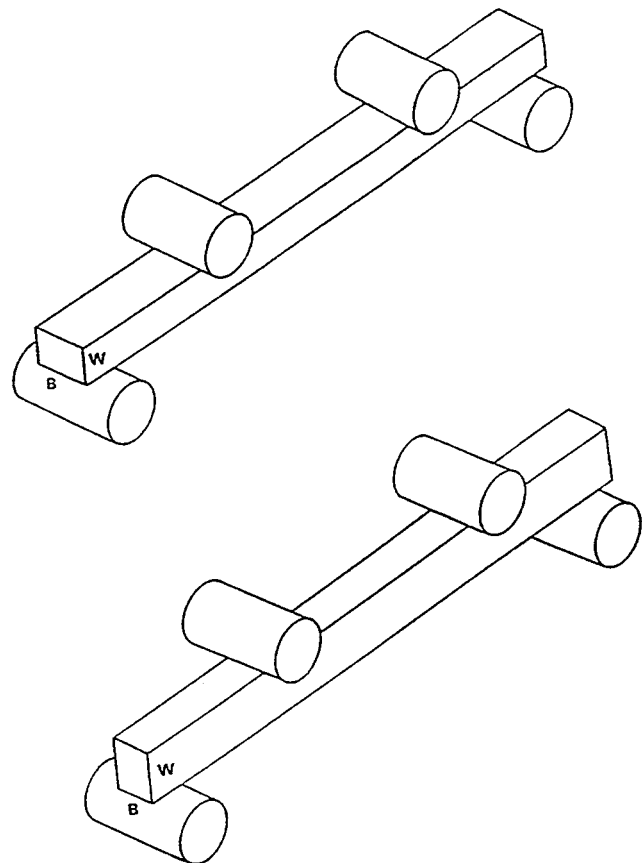
specimen. There also is a potential for introduction of residual stresses. Machine grinding will be necessary for very hard ceramics. If machine grinding is used, use fine wheel grits and small removal rates.

A3.3.2.7 If water or a cutting fluid is used, then ensure that the test specimen is dry (for example, by heating) prior to fracture testing.

A3.3.2.8 Annealing or heat treating to remove the residual stresses under the indent are not permitted by this standard due to the risk of crack tip blunting, crack healing, or possible changes in the microstructure.

A3.3.2.9 Measure and record the final (post-polishing) test specimen dimensions,  $B$  and  $W$ , in the vicinity of the precrack to within 0.002 mm.

A3.3.3 *Fracture Test*—Insert the test specimen into the test fixture as shown in Fig. A3.5, with the surface crack on the tension face, within 1.0 mm of the midpoint between the two inner rollers,  $S_p$ , of the four-point test fixture. Full length test specimens (45 to 50 mm length) should be tested on 20 mm X 40 mm test fixtures and half length test specimens (~25 mm length) should be tested on 10 mm X 20 mm test fixtures. The test specimen may be preloaded to approximately 25 % of the expected fracture force. Place cotton, crumbled tissue, or other appropriate material under the test specimen to prevent the pieces from impacting the fixture upon fracture. Place a thin shield around the fixture to ensure operator safety and to



NOTE 1—The precrack must be on the tension (bottom) surface.

**FIG. A3.5 The Flexure Specimen Can be Tested with Either the Wide or Narrow Face on the Flexure Rollers**



preserve the primary fracture pieces for subsequent fracture analysis. Test the test specimen to fracture at rates in accordance with 9.7.

**NOTE A3.12**—The force rate will range from 10 to 250 N/s for a test specimen with  $B=4$  mm,  $W=3$  mm, with a precrack size,  $a$ , of 100  $\mu\text{m}$ , on a four-point test fixture with  $S_o = 40$  mm. If the test specimen is tested on edge ( $B = 3$  mm,  $W = 4$  mm), the rates will be 13 - 388 N/s. Rates for alternative geometries and precrack sizes can be estimated from Eq A3.9 with an approximation of  $Y = 1.3$ . Displacement rates of 0.002 to 0.10 mm/s will be suitable for a 3 by 4-mm test specimen with a 100  $\mu\text{m}$  precrack in the 4-mm ( $B$ ) face.

**A3.3.4 Post Test Measurements**—Examine the fracture surfaces of the test specimen and measure the initial precrack dimensions,  $a$  and  $2c$ , as shown in Fig. 5 and Fig. A3.3.

**NOTE A3.13**—Fractographic techniques and fractographic skills are needed for this step. The optimum procedure will vary from material to material. Either an optical microscope or a scanning electron microscope can be used. Low magnifications ( $\sim 50$ -100 $\times$ ) can be used to locate the precrack, and intermediate magnifications (300-500 $\times$ ) to photograph the precrack for measurement. If an optical microscope is used, then variation of the lighting source and direction can be used to highlight the precrack. A stage micrometer shall be used to confirm the magnifications. If a scanning electron microscope is used, then it is recommended that a SEM magnification calibration standard be used to confirm the magnification. In some instances dye penetrants may be useful, but care should be taken to ensure that the dyes are completely dry during the fracture test to preclude undesired slow crack growth or undesired crack face bonding. Additional details on techniques to find and characterize the precracks are given in Appendix X1 and Appendix X2 and Ref (24).

### A3.4 Calculation

**A3.4.1** Calculate the stress intensity shape factor coefficients for both the deepest point of the precrack periphery,  $Y_d$ , and for the point at the surface,  $Y_s$ , which will give a maximum error of 3 % for an “ideal” precrack and an estimated maximum error of 5 % for a “realistic” precrack.

**NOTE A3.14**—The stress intensity factor coefficients are from Newman and Raju, Ref (25), and are the same as those used in Practice E 740. These coefficients are valid only for  $a/c \leq 1$ . They can be used for  $a/c$  ratios slightly greater than 1 with a slight loss of accuracy.

**A3.4.1.1** For the deepest point of the precrack:

$$Y_d = \frac{[\sqrt{\pi} M H_2]}{\sqrt{Q}} \quad (\text{A3.2})$$

where:

$$Q = Q(a/c) = 1 + 1.464[a/c]^{1.65} \quad (\text{A3.3})$$

$$M = M(a/c, a/W) = [1.13 - 0.09[a/c]] + \left[ -0.54 + \frac{0.89}{[0.2 + [a/c]]} \right] [a/W]^2 \quad (\text{A3.4})$$

$$H_2 = H_2(a/c, a/W) = 1 - [1.22 + 0.12[a/c]] [a/W] + \left[ 0.5 - \frac{1}{[0.65 + [a/c]]} + 14[1 - a/c]^{24} \right] [a/W]^4 \quad (\text{A3.5})$$

**A3.4.1.2** For the point at the surface:

$$Y_s = \frac{[\sqrt{\pi} M H_1 S]}{\sqrt{Q}} \quad (\text{A3.6})$$

where:

$$H_1 = H_1(a/c, a/W) = 1 - [0.34 + 0.11[a/c]] [a/W] \quad (\text{A3.7})$$

$$S = S(a/c, a/W) = [1.1 + 0.35[a/W]^2] \sqrt{a/c} \quad (\text{A3.8})$$

**Example**—For  $W=3 \times 10^{-3}$  m,  $a=50 \times 10^{-6}$  m and  $2c=120 \times 10^{-6}$  m

$a/c=0.833$ ,  $a/W=0.017$ ,  $Y_d=1.267$  and  $Y_s=1.292$

**A3.4.1.3** If the test specimens are chamfered, and if the chamfer sizes are larger than 0.15 mm, then the fracture toughness values should be corrected in accordance with Appendix X4.

**A3.4.2** For the sc method, use the greater value of  $Y_d$  or  $Y_s$  for  $Y$  and then calculate the fracture toughness,  $K_{Isc}$ , from the following equation:

$$K_{Isc} = Y \left[ \frac{3P_{\max}[S_o - S_i]10^{-6}}{2BW^2} \right] \sqrt{a} \quad (\text{A3.9})$$

where:

- $K_{Isc}$  = the fracture toughness (MPa  $\sqrt{\text{m}}$ ),
- $Y$  = the stress intensity factor coefficient (dimensionless),
- $P_{\max}$  = the maximum force (break force) as determined in 9.8.1 (N),
- $S_o$  = the outer span (m),
- $S_i$  = the inner span (m),
- $B$  = the side to side dimension of the test specimen perpendicular to the crack length (depth) as shown in Fig. 5 (m),
- $W$  = the top to bottom dimension of the test specimen parallel to the crack length (depth) as shown in Fig. 5 (m),
- $a$  = the crack depth (m), and
- $c$  = the crack half width (m).

**NOTE A3.15**—The term in brackets in Eq A3.9 is the flexural strength (in MPa) of the beam with a surface crack. It is often useful to compare this value with the range of values of the flexural strength of test specimens without a precrack, in which fracture occurs from the natural fracture sources in the material.

### A3.5 Requirements

**A3.5.1** The use of the semi-ellipse to model the precrack shape is an approximation which is most valid for instances where the greatest stress intensity factor coefficient is at the deepest part of the precrack ( $Y_{\max} = Y_d$ ). If the maximum stress intensity factor coefficient is at the surface ( $Y_{\max} = Y_s$ ), then the semi-ellipse may not necessarily be an adequate model of the precrack. In such a case, re-examine the precrack shape. If the precrack is not semi-elliptical, reject the datum.

**A3.5.2** If the precrack form is severely distorted in the third dimension (i.e. is not flat), or the form of the precrack is incomplete over more than 33 % of its periphery, reject the datum.

**A3.5.3** If hand grinding or machining damage (see A3.3.2) interfere with the determination of the precrack shape and  $Y_s$  is greater than  $Y_d$ , then reject the datum.

**A3.5.4** If the precrack shows evidence of excessive extension (corner pop-in) at the intersection of the surface, then reject the datum (see example in X2.1)

**A3.5.5** If the precrack shows evidence of stable extension prior to instability, then measure both the initial precrack size, and the critical crack size. Report both the apparent fracture

toughness using the initial precrack size,  $K_{Isc}$ , and the apparent fracture toughness at instability,  $K_{Isc}^*$ . (See examples in X2.1)

NOTE A3.16—It has been common practice to calculate a nominal fracture toughness value based on the maximum force and the original crack dimensions before testing for use as an aid in interpreting sc test results. This practice is consistent with Practice E 740. If significant stable crack growth occurs, the original crack dimensions may no longer be pertinent. If stable extension is due to environmentally-assisted slow crack growth, the nominal fracture toughness will underestimate  $K_{Isc}$  in the absence of environmental effects. Alternatively, if the stable crack extension is due to rising R-curve behavior, the calculated fracture toughness using the initial precrack size will underestimate the fracture toughness at criticality. If stable crack extension is not significant, the sc fracture toughness will be reasonably constant. This slight change in sc fracture toughness is due in large part to the dependence of fracture toughness on the square root of crack size.

NOTE A3.17—Stable crack extension may manifest itself as a halo around the precrack. See examples in X2.1 and Reference (35) for additional information.

A3.5.6 If there is evidence of environmentally-assisted slow crack growth then it is advisable to run additional tests in an inert environment. Alternatively, additional tests may be done in laboratory ambient conditions at faster or slower test rates than those specified in this standard in order to determine the sensitivity to test rates. Testing rates that differ by two to three orders of magnitude or greater than those specified are recommended. (See 9.3.)

### A3.6 Valid Test

A3.6.1 A valid sc test shall meet the following requirements in addition to the general requirements of this standard (9.2):

A3.6.1.1 Test specimen size (A3.1.1) shall be 3 by 4 mm with tolerances as shown in Fig. A3.1 and the length shall be 45 to 50 mm.

A3.6.1.2 Test specimen preparation (A3.1.2) shall conform to the procedures in A3.1.2.

A3.6.1.3 Precrack (A3.3.1) introduced from a Knoop indent or the alternative procedure with canted Vickers indent (Appendix X3) shall be produced in the middle of the polished surface with the long axis of the indent at right angles to the long axis of the test specimen (A3.3.1.1), shall be semi-elliptical (A3.5.1), shall not be severely distorted or incomplete (A3.5.2), shall not have been affected by removal of the residual stress field and shall not have  $Y_s$  greater than  $Y_d$  (A3.5.3) and shall not show evidence of excessive extension (corner pop-in) at the intersection of the surface (A3.5.4).

A3.6.1.4 Residual stresses associated with the indentation shall be removed in accordance with A3.3.2. Material removal shall not introduce residual stresses or excessive machining damage in the test specimen surface.

### A3.7 Reporting Requirements

A3.7.1 In addition to the general reporting requirements of

10.1, 10.2, and 10.3, report the following for the sc method:

A3.7.1.1 If the maximum for  $Y$  occurred at the test specimen surface ( $Y_s$ ) or at maximum crack depth ( $Y_d$ ),

A3.7.1.2 The precrack indent force,  $F$ ,

A3.7.1.3 If there is evidence for stable crack extension, then state such in the report and report both  $K_{Isc}^*$  and  $K_{Isc}$  (A3.5.5),

A3.7.1.4 The fractographic equipment (optical or SEM) used to observe and measure the precrack, fractographic observations, and a photograph of a representative sc precrack, and

A3.7.1.5 The average indentation diagonal length, the procedure used to remove the indentation and residual stress zones, and the depth of material removed.

### A3.8 Precision and Bias

A3.8.1 *Precision*—The precision of the sc method will depend primarily upon the accuracy and precision of measurement of the precrack size. The flexure strength is estimated to be accurate to within 2 to 3 % if the procedures of Test Method C 1161 are followed. The stress intensity shape factors for the precracks are expected to be within 3 to 5 % for the instances where fracture initiates at the deepest point of the precrack periphery. Precrack sizes can be measured to within 5 % with either optical or electron microscopy provided that the material is conducive to fractographic interpretation. Uncertainties in precrack size,  $a$  and  $2c$ , are partially ameliorated by an offsetting influence of the stress intensity factor coefficient,  $Y$ , as discussed in detail in Refs (14) and (26). For a material that fractures from the deepest part of the precrack, and which has a clearly visible, well-shaped precrack, the precision of the sc method is expected to be  $\pm 5$  %.

A3.8.2 Results from a twenty-laboratory round robin organized under the auspices of the VAMAS project can be found in Ref (14). Three ceramics were tested with five replicate tests specified per condition and material. The grand mean for 107 hot-pressed silicon nitride test specimens tested by all 20 laboratories was  $4.59 \text{ MPa } \sqrt{m}$  with a standard deviation of  $0.37 \text{ MPa } \sqrt{m}$ . All test specimens were from a single billet ("E"). The grand mean for 105 hot isopressed silicon nitride tested by 16 laboratories was  $4.95 \text{ MPa } \sqrt{m}$  with a standard deviation of  $0.55 \text{ MPa } \sqrt{m}$ . The grand mean for 33 test specimens of a yttria stabilized zirconia tested by eight laboratories was  $4.36 \text{ MPa } \sqrt{m}$  with a standard deviation of  $0.44 \text{ MPa } \sqrt{m}$ . (The modified-indentation precracking procedure using a Vickers indenter as described in Appendix X3 was used for the latter material.)

A3.8.3 The VAMAS round robin results were analyzed in accordance with Practices E 177 and E 691 to evaluate precision. The results are given in Table A3.1.

TABLE A3.1 Surface Crack in Flexure Results from VAMAS Round Robin (14)

Material	Number of Laboratories	Total Number of Test Specimens	Overall Mean MPa√m <sup>A</sup>	Overall Std Dev MPa√m <sup>A</sup>	Repeatability (Within-Laboratory)			Reproducibility (Between-Laboratories)		
					Std Dev MPa√m	95 %limit MPa√m	COV % <sup>B</sup>	Std Dev MPa√m	95 %limit MPa√m	COV % <sup>B</sup>
Hot-pressed silicon nitride <sup>C</sup>	19	102	4.56	0.32	0.24	0.68	5.4	0.31	0.86	6.8
Hot-isopressed silicon nitride <sup>C</sup>	15	100	5.00	0.48	0.38	1.07	7.7	0.45	1.25	8.9
Yttria-stabilized zirconia <sup>C</sup>	7	29	4.47	0.31	0.29	0.83	6.6	0.29	0.83	6.6

<sup>A</sup>Average and standard deviation of all individual test results combined.

<sup>B</sup>Coefficient of variation.

<sup>C</sup>A data set from a single outlier laboratory set was excluded and accounts for a small difference in the numbers quoted in A3.8.2.

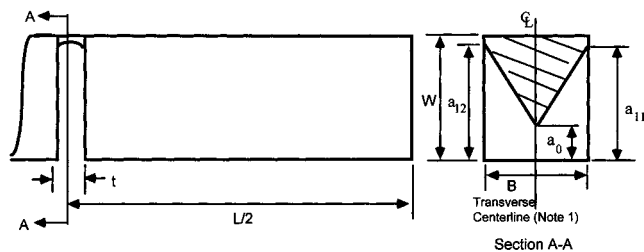
#### A4. SPECIAL REQUIREMENTS FOR THE CHEVRON NOTCH FLEXURE METHOD

##### A4.1 Test Specimen

**A4.1.1 Test Specimen Size**—The test specimen has four acceptable geometries as listed in Fig. A4.1 and as shown in Fig. A4.2.

**NOTE A4.1**—Because no generalized, parametric error and sensitivity analysis studies have been conducted on chevron-notched test specimen geometries, this test method focuses on established geometries which reflect a base of experience (that is, those geometries that have been successfully used, studied, and applied under a range of conditions to a variety of materials).

**A4.1.2 Test Specimen Preparation**—Test specimens prepared in accordance with the Procedure of Test Method C 1161



Configuration and test fixture	L (mm)	B (mm)	W (mm)	a <sub>0</sub> (mm)	a <sub>1</sub> and a <sub>2</sub>	t (mm)
A (Four-point)	45 (min)	3.00±0.13	4.00±0.13	0.80±0.07	0.95W to 1.00W (no overcut)	≤0.25
B (Three-point)	45 (min)	6.35±0.13	6.35±0.13	2.54±0.07	0.95W to 1.00W (no overcut)	≤0.25
C (Four-point)	45 (min)	3.00±0.13	6.00±0.13	1.20±0.07	4.20±0.07 mm	≤0.25
D (Four-point)	45 (min)	3.00±0.13	4.00±0.13	1.40±0.07	0.95W to 1.00W (no overcut)	≤0.25

Note 1—Tip of chevron on transverse centerline shall be within 0.02B.

Note 2—Lengths a<sub>1</sub> and a<sub>2</sub> shall be within 0.02W. No overcut of the notch into the topside of the specimen is allowed.

Note 3—Planes from either side of beam which form the chevron shall meet within 0.3t

Note 4—Allowable ranges for a<sub>1</sub> and a<sub>2</sub> are in terms of W for Configurations A, B and D and but are given in mm for Configuration C.

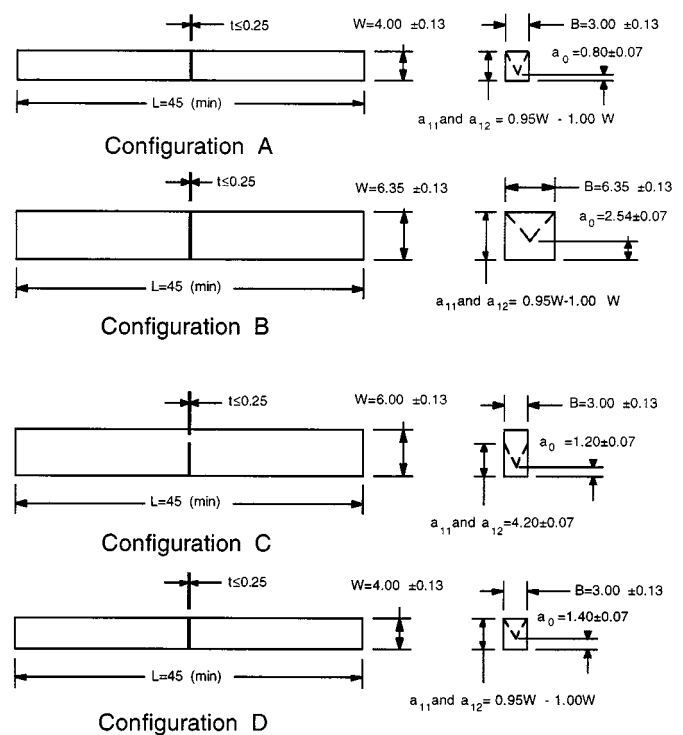
**NOTE 1**—Tip of chevron on transverse centerline shall be within 0.02B.

**NOTE 2**—Lengths a<sub>1</sub> and a<sub>2</sub> shall be within 0.02W. No overcut of the notch into the topside of the test specimen is allowed.

**NOTE 3**—Planes from either side of beam which form the chevron shall meet within 0.3t

**NOTE 4**—Allowable ranges for a<sub>1</sub> and a<sub>2</sub> are in terms of W for Configurations A, B and D and but are given in mm for Configuration C.

FIG. A4.1 Chevron Notch Flexure (vb) Test Specimen Standard Proportions and Tolerances



**NOTE 1**—All dimensions in mm.

**NOTE 2**—Tips of chevrons on transverse centerline within 0.02 B.

**NOTE 3**—Planes on either side which form chevrons shall meet within 0.3t.

FIG. A4.2 Illustrations of Chevron Notch Flexure (vb) Test Specimen Geometries

are suitable as summarized in A4.1.2.1-A4.1.2.3. Any alternative procedure that is deemed more efficient may be utilized provided that unwanted machining damage and residual stresses are minimized. Report any alternative test specimen preparation procedure in the test report.

**A4.1.2.1** All grinding shall be done with an ample supply of appropriate filtered coolant to keep workpiece and wheel constantly flooded and particles flushed. Grinding shall be in at least two stages, ranging from coarse to fine rates of material removal. All machining shall be in the surface grinding mode parallel to the test specimen long axis. No Blanchard or rotary

grinding shall be used. The stock removal rate shall not exceed 0.02 mm per pass to the last 0.06 mm per face.

NOTE A4.2—These conditions are intended to minimize machining damage or surface residual stresses which can interfere with tests. As the grinding method of Test Method C 1161 is well established and economical, it is recommended.

A4.1.2.2 Perform finish grinding with a diamond-grit wheel of 320 grit or finer. No less than 0.06 mm per face shall be removed during the final finishing phase, and at a rate of not more than 0.002 mm per pass.

A4.1.2.3 The two end faces need not be precision machined. No edge treatment (that is, chamfering) of longitudinal edges is allowed on the compression face.

A4.1.3 *Chevron Notch*—Cut the chevron notch using a 320 diamond-grit wheel at a rate of not more than 0.002 mm per pass for the final 0.06 mm. The notch thickness,  $t$ , should be slightly V-shaped and should be less than 0.25 mm at any point of its intersection with the surface and should be less than 0.150 mm at the root radius of the chevron. (See also requirements in Fig. A4.1 and Fig. A4.2). Planes of notches cut from each side of the test specimen shall meet within 0.3  $t$ . The tip of the chevron shall be on center within 0.02  $B$ .

NOTE A4.3—Use of special machining fixtures for producing chevron notches have been shown to reduce machining costs while increasing the incidence of consistent chevron notches (27).

NOTE A4.4—Larger notch thicknesses are acceptable provided that stable crack extension occurs. A V-shaped notch (larger notch width where it intersects the test specimen surface than at the root of the notch) rather than a straight notch shape has resulted in more consistent results (23).

NOTE A4.5—Because no generalized, parametric error and sensitivity analysis studies have been conducted on chevron notch geometries, the notch tolerances given represent those commonly achieved under commercial machining conditions on chevron-notched test specimens which were ultimately used in valid fracture tests (31).

A4.1.4 Prepare at least ten test specimens. This will provide extra test specimens to determine if stable crack growth can be attained without extra preparation (A4.4.1).

## A4.2 Apparatus

A4.2.1 *General*—This test is conducted in three- or four-point flexure. A displacement measurement (or estimate of displacement from a time sweep) is required.

A4.2.2 *Fracture Test Fixture*—The general principles of three- and four-point test fixtures are detailed in 7.4 and illustrated in Fig. A1.1 and Fig. A1.2, respectively. For four-point flexure the outer and inner spans are  $S_o = 40$  mm and  $S_i = 20$  mm, respectively. For three-point flexure the support span is  $S_o = 38$ -40 mm.

## A4.3 Procedure

A4.3.1 *Test Specimen Measurement and Alignment*—In general, measure and align the test specimen according to 9.5 and 9.6. Measure the notch dimension,  $a_o$ , from the chevron tip to the test specimen surface at the notch mouth (that is, opposite the tip of the chevron). Measure the notch dimensions,  $a_{11}$  and  $a_{12}$ , where the notch groove meets the test specimen surface and calculate  $a_1$ , the average of the two values. The difference between the average and the individual values shall be no more than 0.02  $W$ . Orient the chevron tip toward the

outer span (that is, the tip of the chevron section is toward the tensile surface). Align the chevron notch with the centerline of the middle roller in the three-point flexure fixture within 0.5 mm or within 1.0 mm of the midpoint between the two inner rollers,  $S_p$ , of the four-point flexure fixture.

A4.3.2 *Test Record*—Select a combination of load-sensing device and recording device such that the forces can be obtained from the test record within an accuracy of 1 %. Either load-point displacement, actuator displacement (stroke), displacement of the test specimen at the notch plane, back-face strain or time can be used.

NOTE A4.6—For autographic recording devices choose the sensitivities of force (y-axis) and displacement or time (x-axis) to produce an initial elastic loading trace with a slope between 0.7 and 1.5 (ideally a slope of 1.0) so as to provide a good indication of stable crack growth.

A4.3.3 *Test Rate*—Test the test specimen to fracture at actuator displacement (stroke) rates between 0.0005 to 0.005 mm/s for all the configurations.

A4.3.4 *Post Test Measurements*—Examine the chevron notch at sufficient magnification ( $\sim 30\times$ ). The tip of the chevron shall be on center within 0.02  $B$ , and the centerline of the notch grooves on either side of the tip shall meet within 0.3  $t$ .

A4.3.5 Examine the fracture surface to determine how well the crack followed the chevron notch plane and separated the test specimen into two pieces. If the “crack follow” through the chevron section was poor, the crack will have deviated substantially farther into one half than the other. If the actual crack surface deviates severely from the intended crack plane as defined by the chevron notch plane, then the test may be invalid.

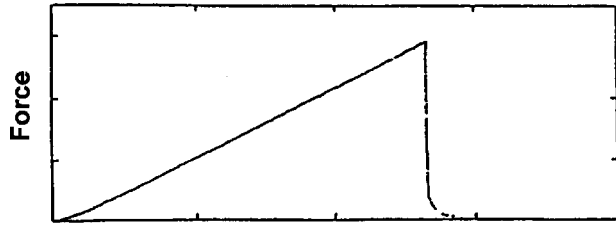
NOTE A4.7—Deviation of the crack from the notch plane can result from one or more of the following:

- (a) Strong anisotropy, in which the fracture toughness in the intended crack plane is substantially larger than the fracture toughness in another crack orientation.
- (b) Coarse-grained or heterogeneous materials.
- (c) Misalignment of the test specimen in the fixture or an out-of-specification notch.

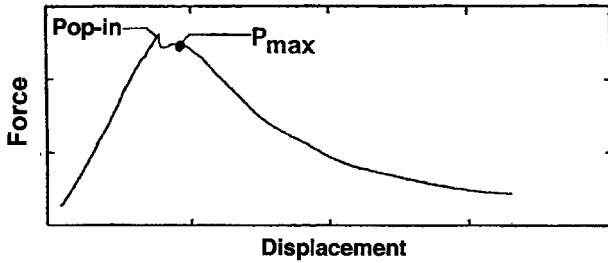
A4.3.6 *Post Test Interpretation*—The test record shall exhibit a smooth (nonlinear) transition through the maximum force prior to final fracture. If the test specimen exhibits a sudden drop in force from the initial linear portion for the test record not followed by a subsequent force increase, the test is unstable and invalid (See Fig. A4.3a). Determine the relevant maximum test force,  $P_{max}$ , from the test record. In some cases the test specimen will overload slightly at crack initiation, as shown in Fig. A4.3b. In the calculations, use the maximum stable force marked  $P_{max}$  in Fig. A4.3b and Fig. A4.3c.

A4.3.6.1 If there is evidence of environmentally-assisted slow crack growth then it is advisable to run additional tests in an inert environment. Alternatively, additional tests may be done in laboratory ambient conditions at faster or slower test rates than those specified in this standard in order to determine the sensitivity to test rates. Testing rates that differ by two to three orders of magnitude or greater than those specified are recommended. (See 9.3.) However, at actuator displacement rates greater than 0.008 mm/s, stability may be difficult to detect.

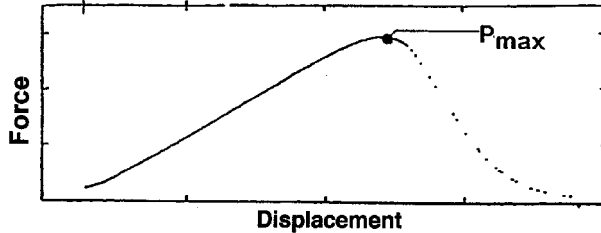




a) Unstable fracture from a chevron notch tip (invalid result) [34]



(b) Overloading prior to crack initiation followed by stable extension [15]



(c) Stable crack extension through maximum load [34]

**FIG. A4.3 Illustrative Applied Force-Displacement Curves: (a) Unstable Fracture from Chevron Tip (34) (Invalid), (b) Overloading Prior to Crack Initiation Followed by Stable Extension (15) and (c) Stable Crack Extension Through Maximum Force (34)**

#### A4.4 Recommendations

A4.4.1 In some instances a stable crack will not initiate from the tip of the chevron, resulting in test specimen overload (that is, a force greater than that to produce stable fracture) or underload (that is, a force less than that to produce stable fracture) and catastrophic fracture from the chevron tip, Fig. A4.3a. If this occurs, a simple compression-compression fatiguing procedure to damage the chevron tip, thereby promoting stable initiation and growth of a crack, can be used. The test specimen is placed in the test fixture upside down and the crack tip loaded in compression, several times, to approximately three times the estimated fracture force expected for the normal position. On unloading, remove the test specimen and test it as specified in A4.3.

A4.4.2 Machining of the chevron notch can influence the scatter in the results. Thinner, or more precise notch thicknesses seem to decrease scatter and initiate stable crack growth more readily (15, 28, 29, 30). The notch thickness,  $t$ , should be in accordance with A4.1.3.

A4.4.3 Actuator displacement (stroke) may not be as sensitive to changes of fracture behavior in the test specimen as measurements taken on the test specimen itself, such as back-face strain, load-point displacement, or displacement at the crack plane (10). In very stiff materials, use of back-face strain is recommended for detection of stable fracture.

#### A4.5 Calculation

A4.5.1 Calculate the fracture toughness,  $K_{Ivb}$ , from the following equation:

$$K_{Ivb} = Y_{\min}^* \left[ \frac{P_{\max} [S_o - S_i] 10^{-6}}{BW^{3/2}} \right] \quad (\text{A4.1})$$

where:

$K_{Ivb}$

= the fracture toughness (MPa  $\sqrt{\text{m}}$ ),

$Y_{\min}^* = Y_{\min}^*(a_o/W, a_1/W)$

= the minimum stress intensity factor coefficient as determined from Eq A4.2, Eq A4.3, Eq A4.4 and Eq A4.5 for test specimen geometries A, B, C, and D, respectively (dimensionless),

$P_{\max}$

= the relevant maximum force as determined in 9.8.2 and A4.3.6 and Fig. A4.3 (N),

$S_o$

= the outer span (m),

$S_i$

= the inner span (m),

$B$

= the side to side dimension of the test specimen perpendicular to the crack length (depth) as shown in Fig. 6 (m),

$W$

= the top to bottom dimension of the test specimen parallel to the crack length (depth) as shown in Fig. 6 (m).

A4.5.1.1 The stress intensity factor coefficient,  $Y_{\min}^*$ , for geometry A and four-point flexure as derived using a straight through crack assumption and a subsequent curve fit of its relation to  $a_o/W$  and  $a_1/W$  (31, 32) is given as:

$$Y_{\min}^* = \quad (\text{A4.2})$$

$$Y_{\min}^*(a_o/W, a_1/W) =$$

$$\frac{0.3874 - 3.0919(a_o/W) + 4.2017(a_1/W) - 2.3127(a_1/W)^2 + 0.6379(a_1/W)^3}{1.0000 - 2.9686(a_o/W) + 3.5056(a_o/W)^2 - 2.1374(a_o/W)^3 + 0.0130(a_1/W)}$$

for  $0.177 \leq a_o/W \leq 0.225$  and  $0.950 \leq a_1/W < 1.000$  and a maximum error of 1 %.

**Example**—For  $W = 4.00 \text{ mm} = 4.00 \times 10^{-3} \text{ m}$ ,  $a_o = 0.80 \text{ mm} = 0.80 \times 10^{-3} \text{ m}$  and

$a_1 = 4.00 \text{ mm} = 4.00 \times 10^{-3} \text{ m}$  then

$a_o/W = 0.20$ ,  $a_1/W = 1.00$ ,  $Y_{\min}^* = 4.23$ .

A4.5.1.2 The stress intensity factor coefficient,  $Y_{\min}^*$ , for geometry B and three-point flexure as derived using straight through crack assumption and a subsequent curve fit of its relation to  $a_o/W$  and  $a_1/W$  (31, 32) is given as:

$$Y_{\min}^* = \quad (\text{A4.3})$$

$$Y_{\min}^*(a_o/W, a_1/W) =$$

$$\frac{0.7601 - 3.6364(a_o/W) + 3.1165(a_1/W) - 1.2782(a_1/W)^2 + 0.3609(a_1/W)^3}{1.0000 - 3.1199(a_o/W) + 3.0558(a_o/W)^2 - 1.0390(a_o/W)^3 + 0.0608(a_1/W)}$$

for  $0.382 \leq a_o/W \leq 0.420$  and  $0.950 \leq a_1/W < 1.00$  and a maximum error of 1 %

*Example*—For  $W = 6.35 \text{ mm} = 6.35 \times 10^{-3} \text{ m}$ ,  $a_o = 2.54 \text{ mm} = 2.54 \times 10^{-3} \text{ m}$  and  $a_1 = 6.35 \text{ mm} = 6.35 \times 10^{-3} \text{ m}$  then  $a_o/W = 0.40$ ,  $a_1/W = 1.00$ ,  $Y^*_{\min} = 6.40$ .

A4.5.1.3 The stress intensity factor coefficient,  $Y^*_{\min}$ , for geometry C and four-point flexure as derived using Bluhm's slice model and a subsequent curve fit of its relation to  $a_o/W$  and  $a_1/W$  (31, 32, 33) is given as:

$$Y^*_{\min} = \quad (A4.4)$$

$$Y^*_{\min}(a_o/W, a_1/W) =$$

$$\frac{1.4680 + 5.5164(a_o/W) - 5.2737(a_1/W) + 8.4498(a_1/W)^2 - 7.9341(a_1/W)^3}{1.0000 + 3.2755(a_o/W) - 4.3183(a_o/W)^2 + 2.0932(a_o/W)^3 - 1.9892(a_1/W)}$$

for  $0.184 \leq a_o/W \leq 0.216$  and  $0.674 \leq a_1/W \leq 0.727$  and a maximum error of 1 %

*Example*—For  $W = 6.00 \text{ mm} = 6.00 \times 10^{-3} \text{ m}$ ,  $a_o = 1.20 \text{ mm} = 1.20 \times 10^{-3} \text{ m}$  and  $a_1 = 4.20 \text{ mm} = 4.20 \times 10^{-3} \text{ m}$  then  $a_o/W = 0.20$ ,  $a_1/W = 0.70$ ,  $Y^*_{\min} = 2.80$ .

A4.5.1.4 The stress intensity factor coefficient,  $Y^*_{\min}$ , for geometry D and four-point flexure as derived using a straight through crack assumption and a subsequent curve fit of its relation to  $a_o/W$  and  $a_1/W$  (31, 32) is given as:

$$Y^*_{\min} = \quad (A4.5)$$

$$Y^*_{\min}(a_o/W, a_1/W) =$$

$$\frac{0.5256 - 3.4872(a_o/W) + 3.9861(a_1/W) - 2.0038(a_1/W)^2 + 0.5489(a_1/W)^3}{1.0000 - 2.9050(a_o/W) + 2.7174(a_o/W)^2 - 0.8963(a_o/W)^3 + 0.0361(a_1/W)}$$

for  $0.322 \leq a_o/W \leq 0.380$  and  $0.950 \leq a_1/W < 1.000$  and a maximum error of 1 %.

*Example*—For  $W = 4.00 \text{ mm} = 4.00 \times 10^{-3} \text{ m}$ ,  $a_o = 1.40 \text{ mm} = 1.40 \times 10^{-3} \text{ m}$  and

$a_1 = 4.00 \text{ mm} = 4.00 \times 10^{-3} \text{ m}$  then  $a_o/W = 0.35$ ,  $a_1/W = 1.00$ ,  $Y^*_{\min} = 5.85$ .

#### A4.6 Valid Test

A4.6.1 A valid vb test shall meet the following requirements in addition to the general requirements of these test methods (9.2):

A4.6.1.1 Test specimen size (A4.1.1) shall be as listed in Fig. A4.1 and as shown in Fig. A4.2.

A4.6.1.2 Test specimen preparation (A4.1.2) shall conform to the procedures in A4.1.2.

A4.6.1.3 Chevron notch (A4.1.3 and A4.3.4) shall have planes which meet within  $0.3 t$ , the tip of chevron on the transverse centerline shall be within  $0.02 B$ , and the difference between the average of  $a_{11}$  and  $a_{12}$  (that is,  $a_1$ ) and  $a_{11}$  or  $a_{12}$ , or both, shall not be more than  $0.02 W$ .

A4.6.1.4 Test record (applied force-displacement/time curve) (A4.3.6) shall exhibit smooth (nonlinear) transition through the maximum force prior to final fracture which is indicative of stable crack extension.

#### A4.7 Reporting Requirements

A4.7.1 In addition to the general reporting requirements of 10.1, 10.2 and 10.3, report the following for the vb method.

A4.7.2 Each flexure diagram with a statement about stability (A4.3.6).

A4.7.3 Include statements about the validity of the chevron notch (A4.3.4) and the crack plane (A4.3.5).

#### A4.8 Precision and Bias

A4.8.1 The precision and bias of the chevron-notch procedure in this standard is being determined.

## APPENDIXES

### (Nonmandatory Information)

#### X1. PRECRACK CHARACTERIZATION, SURFACE CRACK IN FLEXURE METHOD

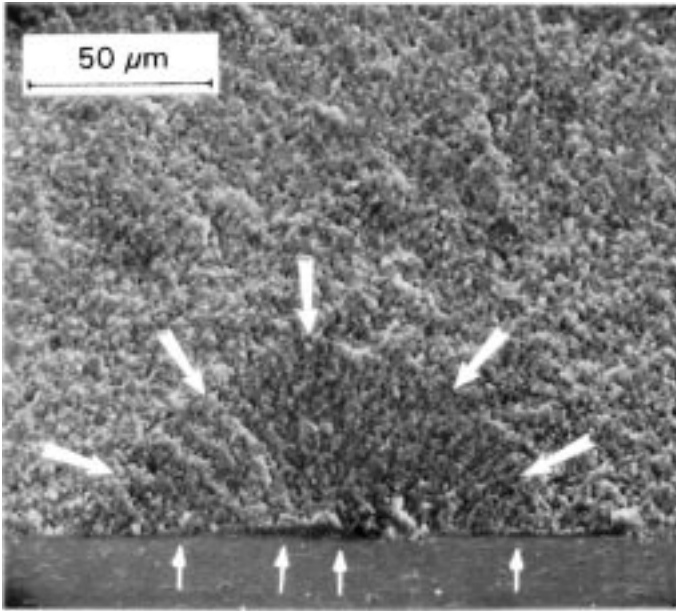
X1.1 The detectability of precracks will vary considerably between ceramic materials. Since precracks are small, of the order  $0.050$  to  $0.200 \text{ mm}$  ( $50$  to  $200 \mu\text{m}$ ) in size, fractographic methods are needed to find and characterize them. Fractographic procedures defined in Practice C 1322 and Ref (24) are suitable. The detectability of precracks depends upon the material, the skill of the fractographer, the type of equipment used, and the familiarity of the examiner with the material. It may be necessary to test 10 test specimens in order to obtain five precracks that are distinct. The best mode of viewing will vary from material to material. Sometimes optical microscopy is adequate, whereas, in other cases, scanning electron microscopy (SEM) is necessary. The magnifications necessary for precrack characterization are usually  $100$  to  $500\times$ . The superior depth of field of the scanning electron microscope is advantageous in many instances.

X1.2 Many ceramic materials have clear fractographic

markings so that the precracks are detectable with either optical or scanning electron microscopy. Examples are shown in Figs. X1.1-X1.4. Fracture toughness measurements on the same test specimens using both optical and scanning electron microscopy precrack measurements are often in good agreement (14, 24). The slight differences in size measurements have only small influences on fracture toughness values, due in large part to the square root dependence of fracture toughness on precrack size.

X1.3 Many coarse-grained or incompletely-densified ceramics are not conducive to fractographic analysis. The se method may not be suitable for these materials, since no meaningful estimate of the precrack size can be made.

X1.4 The precrack is easiest to detect if: 1) it is on a slightly different plane (angle) than the final fracture surface; 2) it fractures in a different mode (transgranular) than the final fracture (intergranular); 3) it leaves an arrest line; 4) it has been



NOTE 1—No material has been removed after indenting, and portions of the Knoop indent are visible (small arrows).

**FIG. X1.1 Knoop Indent Precrack in a Hot-Pressed Silicon Nitride as Photographed in a Scanning Electron Microscope**

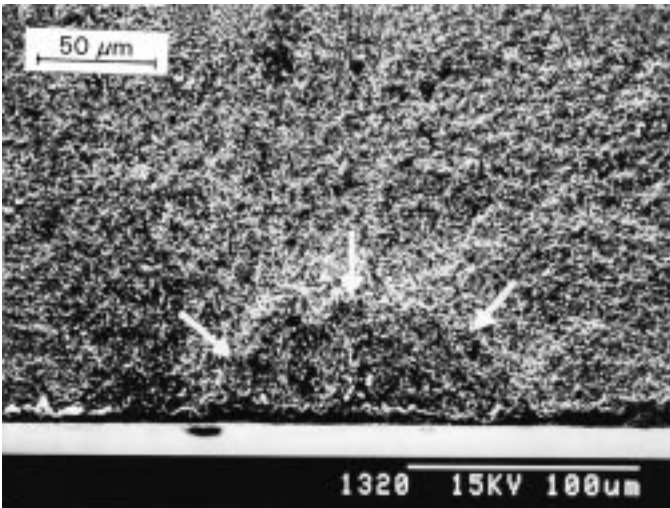
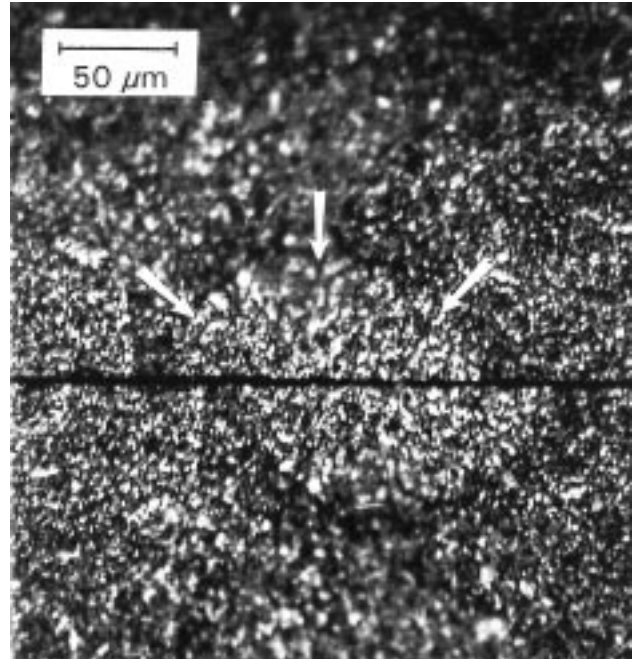


**FIG. X1.2 Knoop Indent Precrack in a Hot-Pressed Silicon Nitride as Photographed in a Scanning Electron Microscope**

dye penetrated or thermally tinted; or 5) it has coarse or fine hackle lines which change direction at the boundary. Conditions 1, 2, or 4 will cause the precrack to have a slightly different reflectivity or contrast than the rest of the fracture surface.

**X1.5** Dye penetration procedures may be beneficial and are permitted by these test methods. Considerable caution should be exercised in the use of these test methods, since it is difficult to completely penetrate the small, tight cracks in ceramics. The optimum penetrant and impregnation procedure will vary between materials. Experience has shown that penetration procedures work best in “white” or light-colored ceramics such as alumina and zirconia. The penetrant should be fully dried



NOTE 1—The precrack is the same as in Fig. X1.2. (Note that both halves of the test specimen are shown “back to back”.)

**FIG. X1.3 Optical Microscope Photograph of a Knoop Precrack in Hot-Pressed Silicon Nitride**

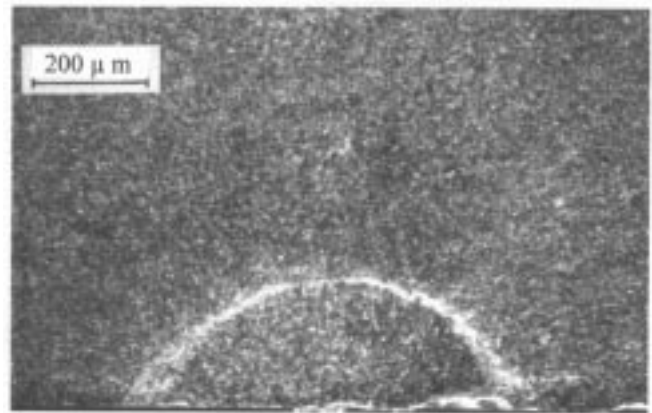


**FIG. X1.4 Knoop Indent Precrack in a 99.9 % Sintered Alumina as Photographed in the Scanning Electron Microscope**

before conducting the fracture test.

**X1.6** Although heat treatments may be useful in highlighting or “tinting” precracks (especially in silicon carbides), this approach shall not be used in this test method since there is a risk of crack healing, crack tip blunting, or microstructural changes. This technique is mentioned here for completeness.

NOTE X1.1—The slightly-oxidized precrack will have a different color or appearance on the fracture surface. The method is not applicable to oxide ceramics or glasses. Optimum temperatures and times vary considerably between materials.

**X1.7** The following paragraphs describe inspection procedures that have been effective in discerning precracks. Additional photographs and details can be found in Refs (14, 24).



X1.8 Both fracture surfaces should be examined. The precrack may be clearer on one surface than the other.

X1.9 Sometimes it is helpful to aim a light source at a low angle to create shadows during optical microscopy. A precrack may have a “halo” seen with either optical or electron microscopy if the crack is tilted. This is due to the different reflectivity of the ridge formed during the crack realignment to the plane of maximum stress during fracture as illustrated in Fig. X1.5. (Such markings may also be due to stable crack extension, in which case interpretation can be difficult. The guidelines of A3.5.5 are to be followed.) Reference (35) has additional information on precrack halos and their interpretation.

X1.10 Fine hackle lines may change direction at a boundary, and can be used to interpret the initial precrack shape as shown in Fig. X1.6. These are discernible usually only in the scanning electron microscope.

X1.11 A combination of low- and high-power microscopy is usually very effective. This is true for both optical and electron microscopy. Lower power (50 to 100 $\times$ ) photographs often illustrate the precracks quite clearly, but contrast at greater magnifications is lost in the optical or electron microscope, or depth of field is lost in the optical microscope. The photograph taken at low magnification is used to find and delineate the precrack, the photograph taken at higher magnification (100 to 500 $\times$ ) is used for measurements of the precrack size.

X1.12 Precracks often have subtle markings which cannot be discerned on scanning electron microscope television monitors. Photography is essential with the scanning electron microscope, and will reveal precracks much better. Thermal prints should be used with caution, since experience has shown that considerable detail and clarity is lost. The thickness of the

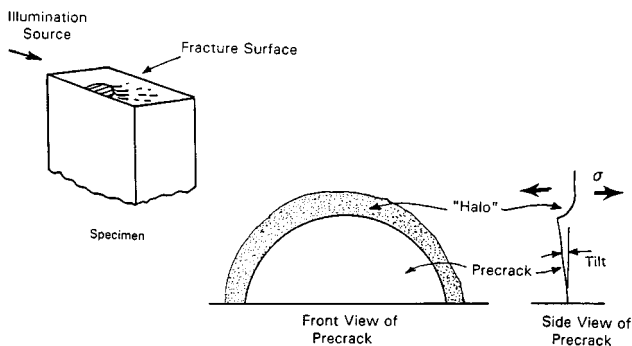


**FIG. X1.5 The Slight Tilt of the Precrack can Create Shadows or Contrast Differences When Viewed in the Optical or Scanning Electron Microscope**



**FIG. X1.6 Fine Hackle Lines may Change Direction at the Precrack Boundary**

conductive coating applied to the fracture surface of the ceramic and the SEM excitation voltage may influence the contrast level between the pre-crack and the fast fracture region.

X1.13 Test specimen tilting (10 to 20°) is effective during either optical and SEM microscopy. (This is distinct from the test specimen tilt of ½° used during indenting). A photograph can be taken which may show the precrack quite clearly when tilted, but cannot be used for measurement due to the foreshortening of the precrack dimensions. A separate photograph taken perpendicular to the fracture surface is made for measurements, and the two photographs are compared to delineate the precrack on the latter photograph.

X1.14 Stereo photography with the scanning electron microscope is extremely effective in detecting the full topography of a precrack, and can often discern precracks quite clearly, when they are undetectable by other means. Take one photograph perpendicular to the precrack, and a second photograph at 10 to 20° off axis at the same magnification. A stereo viewer can be very helpful. Use the pair of photographs to discern the precrack, but take size measurements only from the former photograph.

X1.15 A thin gold-palladium coating, such as is used to coat nonconductive ceramics prior to electron microscope examination, can be very beneficial in optical microscopy on transparent or translucent “white” ceramics. The coating can mask unwanted internal reflections and scatter. Thick gold-palladium coatings are to be avoided during coating prior to scanning electron microscopy since such coatings can obscure fine detail. A  $20 \times 10^{-6}$  mm (20 nm) coating thickness has proved effective for most ceramics. The gold-palladium coating can be applied at a shallow angle (grazing incidence) to the fracture surface. This will promote contrast which will enhance fine detail.

X1.16 In some instances, switching to the backscattering mode in the SEM can enhance detectability.

X1.17 In some cases, simply applying green felt tip marker ink to the fracture surface of the specimens (after fracture) helps outline the precrack. This simple step often works well on translucent or white ceramics.



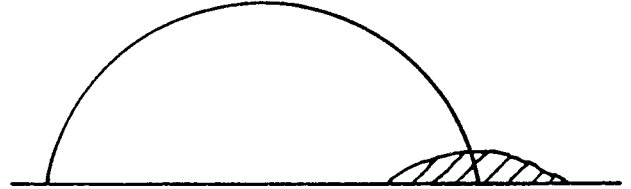
## X2. COMPLICATIONS IN INTERPRETING SURFACE CRACK IN FLEXURE PRECRACKS

X2.1 Precrack interpretation may be complicated by certain features on the fracture surface. The following illustrations

provide guidance in such instances.

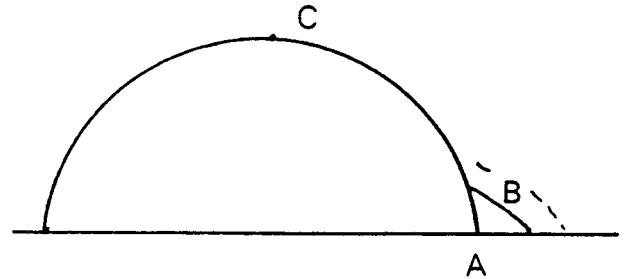
### Hand Grinding or Machining Damage

This can occur if the hand grinding or machining to remove the indent is done too aggressively. Specimens with this damage can be repolished to remove the surface damage. If it is necessary to interpret such precracks, then approximate the semi-ellipse shape as if the surface damage is not present. If the maximum Y factor is at the surface, reject the datum (A3.5.3)



### Corner Pop-in

During the fracture test, the precrack reaches critical fracture condition at Point A first. A small crack extends to B. Final fracture starts at Point C. The original ellipse should be used to compute fracture toughness. If the extension at points A-B is excessive, reject the datum. Hand grind the specimen more to force the  $Y_{max}$  to be at the deepest point,  $Y_d$ . (A3.5.4)



### Poorly Defined Crack at the Surface

This can occur in instances where the precrack and the final fracture crack are on the same plane. (The  $1/2^\circ$  tilt may not have been adequate.) Alternatively, a limited depth of field in the optical microscope may hamper focusing the entire precrack. Estimate or approximate the semi-ellipse shape as best as possible, but if more than 33% of the precrack periphery is not visible, reject the datum. (A3.5.2)

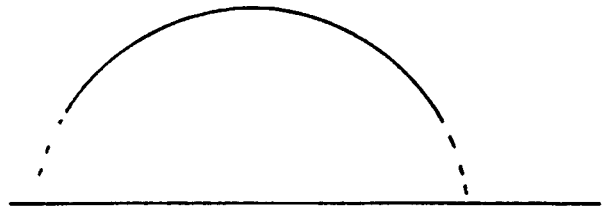
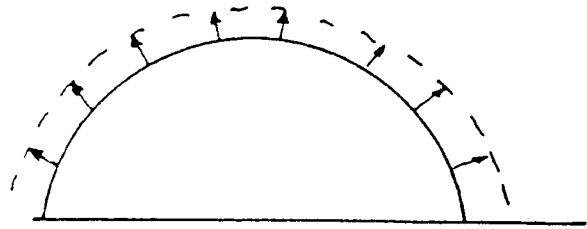


FIG. X2.1 Precrack Interpretations

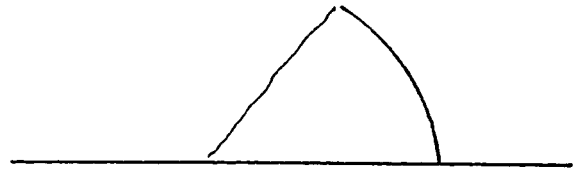
#### Stable Crack Extension

The crack may extend stably prior to fast fracture, either due to rising R-curve behavior, or environmentally-assisted crack growth. This can either be an interference or a useful tool to study the stable crack growth phenomena. Definitive interpretation of such stable crack extension markings on a fracture surface is extremely difficult. If stable crack extension is detected, follow the guidelines in A3.5.5 and A3.5.6.



#### Precrack Truncation

The final crack is on a different plane and intersects only a portion of the precrack. This can occur if the precrack is not perpendicular to the maximum stress in the specimen, and fracture commences from one point on the precrack periphery, but then truncates the remainder of the precrack. In these cases, reject the datum (A3.5.2)



#### Precrack Segmentation

The precrack consists of three segments. The precrack is not flat and has a three-dimensional shape. It is "rippled" or "corrugated" as shown in the figure. The interference may be from lateral or Hertzian cracks associated with the original indent, or it may be due to non-uniform density in the ceramic. (This problem is common in some sintered ceramics.) If the waviness or corrugation is excessive, reject the datum. (A3.5.2)

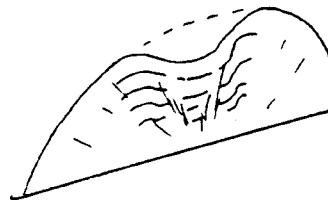
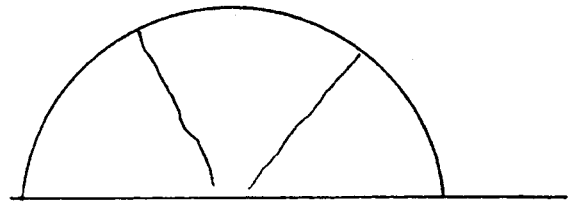


FIG. X2.1 Precrack Interpretations (continued)

### X3. ALTERNATIVE PRECRACKING PROCEDURE, SURFACE CRACK IN FLEXURE METHOD

X3.1 In some very "tough" ceramics, semi-elliptical or semicircular median cracks may not form under a Knoop indent. The precracks may be very shallow and apt to be removed during the subsequent material removal steps. This can occur even if very high indent forces (for example, ~500 N) are used. In such cases, the following alternative precracking procedure may be used.

X3.2 Indent the polished surface of the test specimen with

a Vickers indenter, taking care to orient the indent at right angles (within  $2^\circ$  to the test specimen long axis as shown in Fig. X3.1. Tilt and cant one end of the test specimen  $\frac{1}{2}^\circ$  and  $3^\circ$ , respectively, as shown in Fig. X3.1. Make the indent slightly offset from the transverse center of the test specimen surface as shown in Fig. X3.2b since the precrack that is retained after material removal is on the side of the indent. This procedure will introduce two Palmqvist cracks on the sides of the Vickers

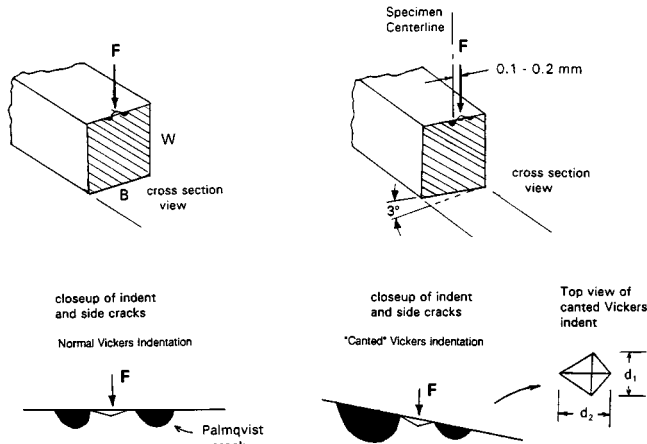
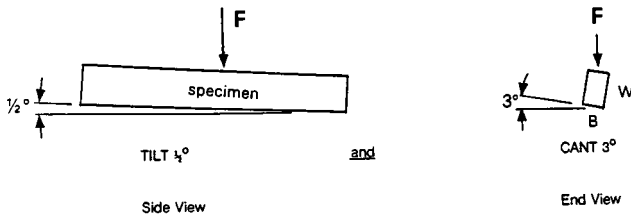


FIG. X3.1 The Alternative Precracking Procedure for a Vickers Indenter Uses Both a Tilt and a Cant to the Test Specimen



(a) Normal Vickers indent (b) Canted Vickers indent

NOTE 1—(a) Shows the Palmqvist type cracks that form on the sides of a normal Vickers indent. (b) Illustrates the cant which enlarges one side crack.

FIG. X3.2 Cross Sectional Views of SC Test Specimens Precracked by the Alternative Procedure for "Tough" Ceramics

indent. The test specimen cant will cause one to be larger than the other. Use a full-force dwell time of 15 s or longer during the indentation cycle.

NOTE X3.1—In some instances such as with zirconia, longer indentation times may be helpful.

X3.3 The indentation force used may have to be determined for each different class of materials through the use of a few trial test specimens. Since this alternative precracking procedure is intended for "tough" materials, greater indentation forces will be necessary (for example, 150 to 200 N is recommended). A single practice test specimen may be indented and broken, without the material removal steps described below in X3.4-X3.8, in order to determine whether a particular indent force is satisfactory.

X3.4 Measure the diagonals for the indent within 0.005 mm (5  $\mu$ m). Calculate the average diagonal length,  $d$ , where  $d=(d_1+d_2)/2$ .

X3.5 Compute the approximate depth of the Vickers indent,  $h$ :

$$h = d/7 \quad (X3.1)$$

X3.6 Measure the test specimen dimension,  $W$ , in the middle of the test specimen to within 0.002 mm. A hand micrometer with a vernier graduation is suitable.

X3.7 Mark the side of the test specimen with a pencil-drawn arrow in order to indicate the surface with the precrack.

X3.8 Remove the indent and the residual stress damage zone under the indent by polishing or hand grinding to a depth of  $2.5h$ . The procedures of A3.3.2.5 or A3.3.2.6 may be used.

NOTE X3.2—Experience has shown that the resultant precracks may be less symmetrical than those formed by the Knoop indenter. The Vickers precrack in canted test specimens may be skewed as shown in Fig. X3.1. Knoop precracks are generally preferable since only one median precrack is formed, rather than multiple Palmqvist or median cracks associated with Vickers indents.

#### X4. Chamfer Correction Factors, Surface Crack in Flexure Method Only

X4.1 The fracture toughness of sc test specimens, Annex A3, should be corrected for corner chamfers if the chamfer size exceeds 0.15 mm. The chamfer size,  $c$ , may be measured with a traveling microscope, photo analysis, or a microscope with a traversing stage. All four chamfers should be measured and an average value used for the correction.

X4.2 The maximum flexural stress may be calculated from simple beam theory and it is common to assume that the cross section is a simple rectangle. The chamfers alter this geometry, however, and the second moment of inertia of the test specimen

cross-section about the neutral axis is altered as discussed in 36. Correction factors,  $F$ , for four equal chamfers are listed in Table X4.1 for test specimens with a 3 mm X 4 mm cross-section size. The factors are practically identical for the two test specimen orientations. The factors are only suitable if there are four chamfers that are of approximately equal size. Fracture toughness then may be corrected:

$$K_{I,scor} = F K_{I,sc} \quad (X3.1)$$

TABLE X4.1 Correction Factor For 3 mm X 4 mm Test Specimens

c (mm)	Correction factor, F B = 4, W = 3	Correction Factor, F B = 3, W = 4
0.080	1.003	1.003
0.090	1.004	1.004
0.100	1.005	1.005
0.110	1.006	1.006
0.120	1.007	1.007
0.130	1.008	1.008
0.140	1.009	1.009
0.150	1.011	1.011
0.160	1.012	1.012
0.170	1.014	1.014
0.180	1.015	1.015
0.190	1.017	1.017
0.200	1.019	1.019
0.210	1.020	1.021
0.220	1.022	1.023
0.230	1.024	1.025
0.240	1.027	1.027
0.250	1.029	1.030

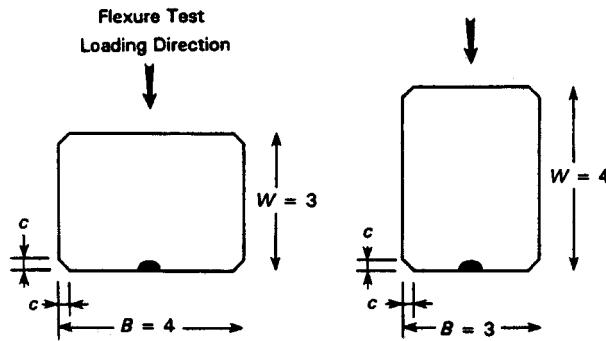


FIG. X4.1 Test Specimen Cross Section

## REFERENCES

- (1) Warren R., and Johanneson, B., "Hard Metals Using 'Bridge Indentation,'" *Powder Metallurgy*, 27, 1984, pp. 25-29.
- (2) Nose T., and Fujii, T., "Evaluation of Fracture Toughness for Ceramic Materials by a Single-Edge-Pre-cracked-Beam Method," *Journal of American Ceramic Society*, 71 [5], 1988, pp. 328-333.
- (3) Petrovic J. J., and Mendiratta, M. G., "Fracture from Controlled Surface Flaws," in *Fracture Mechanics Applied to Brittle Materials*, ASTM STP 678, S. W. Freiman ed., 1979, pp. 83-102.
- (4) Petrovic, J. J., Jacobson, L. A., Talty, P. K., and Vasudevan, A. K., "Controlled Surface Flaws in Hot-Pressed  $\text{Si}_3\text{N}_4$ ," *Journal of American Ceramic Society*, 48 [3-4], 1975, pp. 113-116.
- (5) Munz, D., Bubsey, R. T., and Shannon, Jr. J. L., "Fracture Toughness Determination of  $\text{Al}_2\text{O}_3$  Using Four-Point-Bend Specimens with Straight-Through and Chevron Notches," *Journal of American Ceramic Society*, 63 [5-6], 1980, pp. 300-305.
- (6) Calomino, A. M., Ghosn, L., "Optimum Configurations for the Chevron-Notched Four Point Bend Specimen," *International Journal of Fracture Mechanics*, 72 [4] 1995, pp. 311-320.
- (7) Choi S. R., and Salem, J. A., "Crack-Growth Resistance of In Situ-Toughened Silicon Nitride," *Journal of American Ceramic Society*, 77 [4], 1994, pp. 1042-1046.
- (8) Baratta F. I., and Dunlay, W. A., "Crack Stability in Simply Supported Four-Point and Three-point Loaded Beams of Brittle Materials," *Mechanics of Materials*, 10, 1990, pp. 149-159.
- (9) Bar-On, I., Baratta, F. I., and Cho, K., "Crack Stability and its Effect on Fracture Toughness of Hot Pressed Silicon Nitride Beam Specimens," *Journal of American Ceramic Society*, 79 [9], 1996, pp. 2300-2308.
- (10) Salem, J. A., Ghosn, L. J., and Jenkins, M. G., "Back-Face Strain as a Method for Monitoring Stable Crack Extension," *Ceramic Science and Engineering Proceedings*, Vol. 19, No. 4, pp. 587-594, 1998.
- (11) Mizuno M., and Kon J., "VAMAS Round Robin on Fracture Toughness Measurement of Ceramic Matrix Composite," *VAMAS Technical Report No. 32*, Japan Fine Ceramic Center, Nagoya, Japan, September 1997.
- (12) Baratta F. I., and Fett, T., "The Effect of Load and Crack Misalignment on Stress Intensity Factors for Bend Type Fracture Toughness Specimens," *Journal of Testing Evaluation*, 28 [2] 2000, pp. 96-102.
- (13) Quinn, G. D., Salem, J., Bar-On, I., Cho, K., Foley, M., and Ho Fang, "Fracture Toughness of Advanced Ceramics at Room Temperature," *J. Res. Natl. Stand. Technol.* 97, 1992, pp. 579-590.
- (14) Quinn, G. D., Kübler, J. J., and Gettings, R. J., "Fracture Toughness of Advanced Ceramics by the Surface Crack in Flexure (SCF) Method: A VAMAS Round Robin," *VAMAS Technical Report No. 17*, National Institute of Standards and Technology, Gaithersburg, Maryland, June 1994.



- (15) J.A. Salem, J.L. Shannon, Jr., and M.G. Jenkins, "Some Observations in Fracture Toughness and Fatigue Testing with Chevron-Notched Specimens," in *Chevron-Notch Test Experience: Metals and Non-Metals*, ASTM STP 1172, eds. K.R. Brown and F. I. Baratta, 1992.
- (16) Choi, S. R., Chulya, A., and Salem, J. A., "Analysis of Precracking Parameters for Ceramic Single-Edge-Pre-cracked-Beam Specimens," *Fracture Mechanics of Ceramics*, Vol 10, R.C. Bradt, D.P.H. Hasselman, D. Munz, M. Sakai, and V. Ya. Shevchenko, eds., Plenum Press, New York, 1992, pp. 73-88.
- (17) Bar-On, I., Beals, J. T., Leatherman, G. L., and Murray, C. M., "Fracture Toughness of Ceramic Precracked Bend Bars," *Journal of American Ceramic Society*, 73 [8] 1990, pp. 2519-2522.
- (18) Grendahl, S., Bert, R., Cho, K., and Bar-On I., "Effects of Residual Stress and Loading Geometry on Single Edge Precracked Beam (SEPB) Fracture Toughness Test Results", *Journal of American Ceramic Society*, 73, 83 [10] 2000, pp. 2625-2627.
- (19) Srawley, J. E., "Wide Range Stress Intensity Factor Expressions for ASTM E 399 Standard Fracture Toughness Specimens," *International Journal of Fracture Mechanics*, 12, 1976, pp. 475-485.
- (20) Baratta F. I., to Quinn, G. D., Personal Communication, National Institute for Standards and Technology, September 1996.
- (21) Srawley J. E., and Gross, B., "Side-Cracked Plates Subject to Combined Direct and Bending Forces," *Cracks and Fracture, ASTM STP 601*, 1976, pp. 559-579.
- (22) Awaji, H., Kon, J., Okuda, H., "The VAMAS Fracture Toughness Round-Robin on Ceramics," *VAMAS Technical Report No. 9*, Japan Fine Ceramics Center, Nagoya, Japan, Dec. 1990.
- (23) Awaji, H., Yamada, T., and Okuda, H., "Results of the Round Robin Fracture Toughness Test on Ceramics - VAMAS Project," *Journal of Japanese Ceramic Society*, International Edition, 4, 1991, pp. 403-408.
- (24) Quinn G. D., and Gettings, R. J., "Fractography and the Surface Crack in Flexure (SCF) Method for Evaluating Fracture Toughness of Ceramics," *Ceramic Transactions*, Vol 64, *Third Alfred Conference on Fractography of Glasses and Ceramics*, J.R. Varner, V.D. Frechette, G.D. Quinn, eds., American Ceramic Society, Westerville, Ohio, pp. 107-144, 1996.
- (25) Newman J. C., and Raju, I. S., "An Empirical Stress Intensity Factor Equation for the Surface Crack," *Engineering Fracture Mechanics* 15 [1-2] 1981, pp. 185-192.
- (26) Quinn, G. D., Gettings, R. J., Kubler, J.J., "Fracture Toughness of Ceramics by the Surface Crack in Flexure (SCF) Method," in *Fracture Mechanics of Ceramics*, Vol 11, R.C. Bradt, D.P.H. Hasselman, D. Munz, M. Sakai, and V. Ya. Shevchenko, eds., Plenum Press, New York, 1996, pp. 203-218.
- (27) M. G. Jenkins, T. Chang, and A Okura, "A Simple Machining Jig for Chevron-Notched Specimens," *Experimental Techniques*, 12 [8] 20-22, 1988.
- (28) M. Mizuno and H. Okuda "VAMAS Round Robin on Fracture Toughness of Silicon Nitride at High Temperature," *Technical Report No. 16*, Japan Fine Ceramics Center, Nagoya, Japan, 1993.
- (29) B. J. De Smet, P. W. Bach and P.P.A.C. Pex, "Fracture Toughness Testing of Ceramics," in *Proceedings of the 2nd European Ceramic Society Conference, Augsburg, Germany, Sept. 11-14, 1991*.
- (30) B. J. De Smet and P. W. Bach, "Fracture Toughness Testing of Ceramics," Netherlands Energy Research Foundation, ECN-I-91-070, 1991.
- (31) J.A. Salem, L.J. Ghosn, M.G. Jenkins, and G.D. Quinn, "Stress Intensity Coefficients for Chevron-Notched Flexure Specimens," *Ceramic Engineering and Science Proceedings*, V 20, No. 3, pp. 503-521, 1999.
- (32) J. Salem, L. Ghosn, and M. Jenkins, "Report on Stress Intensity Factor Coefficients for Chevron-Notched Flexure Specimens," Archival Files for C28.01 Task Group on Fracture Toughness of Advanced Ceramics, PS070, ASTM, W. Conshohocken, Pennsylvania, 20 April 1998.
- (33) J. I. Bluhm, "Slice Synthesis of a Three-Dimensional 'Work-of-Fracture' Specimen for Brittle Material," *Engineering Fracture Mechanics*, 7, 593-604, 1975.
- (34) J.A. Salem and S.R. Choi, "Ceramic Technology Bimonthly Progress Report," ORNL CF-94/205, Oak Ridge National Laboratory, Oak Ridge, Tennessee, 1994.
- (35) Swab, J.J. and Quinn, G.D., "Effect of "Halos" on  $K_{Ic}$  Determined by the Surface Crack in Flexure Method," *Journal of American Ceramic Society*, 81 [9] 1998, pp. 2261-2268.
- (36) Baratta, F.I., Quinn, G.D., and Matthews, W.T., "Errors Associated With Flexure Testing of Brittle Materials," U.S. Army Materials Technology Laboratory Technical Report MTL TR 87-35, Watertown, MA 02187, July 1987.

ASTM International takes no position respecting the validity of any patent rights asserted in connection with any item mentioned in this standard. Users of this standard are expressly advised that determination of the validity of any such patent rights, and the risk of infringement of such rights, are entirely their own responsibility.

This standard is subject to revision at any time by the responsible technical committee and must be reviewed every five years and if not revised, either reapproved or withdrawn. Your comments are invited either for revision of this standard or for additional standards and should be addressed to ASTM International Headquarters. Your comments will receive careful consideration at a meeting of the responsible technical committee, which you may attend. If you feel that your comments have not received a fair hearing you should make your views known to the ASTM Committee on Standards, at the address shown below.

This standard is copyrighted by ASTM International, 100 Barr Harbor Drive, PO Box C700, West Conshohocken, PA 19428-2959, United States. Individual reprints (single or multiple copies) of this standard may be obtained by contacting ASTM at the above address or at 610-832-9585 (phone), 610-832-9555 (fax), or [service@astm.org](mailto:service@astm.org) (e-mail); or through the ASTM website ([www.astm.org](http://www.astm.org)).